Marine Pollution Bulletin 199 (2024) 115965

Contents lists available at ScienceDirect

Marine Pollution Bulletin

journal homepage: www.elsevier.com/locate/marpolbul

In-situ comparison of high-order detonations and low-order deflagration methodologies for underwater unexploded ordnance (UXO) disposal

Paul A. Lepper [a,*], Sei-Him Cheong [b], Stephen P. Robinson [b], Lian Wang [b], Jakob Tougaard [c], Emily T. Griffiths [c], John P. Hartley [d]

[a] Loughborough University, Loughborough LE11 3TU, UK
[b] National Physical Laboratory, Hampton Road, Teddington TW11 0LW, UK
[c] Aarhus University, 8000 Aarhus, Denmark
[d] Hartley Anderson Ltd, Aberdeen AB11 5BE, UK

ARTICLE INFO

Keywords:
UXO
Detonation
Deflagration
Noise
Seabed vibration
Pollution

ABSTRACT

The unexploded ordnance (UXO) on the seabed off Northwest Europe poses a hazard to offshore developments such as windfarms. The traditional removal method is through high-order detonation of a donor explosive charge placed adjacent to the UXO, which poses a risk of injury or death to marine mammals and other fauna from the high sound levels produced and is destructive to the seabed. This paper describes a sea-trial in the Danish Great Belt to compare the sound produced by high-order detonations with that produced by deflagration, a low-order disposal method that offers reduced environmental impact from noise. The results demonstrate a substantial reduction over high-order detonation, with the peak sound pressure level and sound exposure level being around 20 dB lower for the deflagration. The damage to the seabed was also considerably reduced for deflagration, although there was some evidence for residues of explosives related chemicals in sediments.

1. Introduction

The unexploded ordnance (UXO) that litters the seabed of Northwest Europe poses a hazard to fishing activities and offshore developments such as offshore windfarms. The location and spatial scale of many developments and cable and interconnector projects means there is a high potential to encounter UXO during construction, particularly where there is overlap with World War I and World War II conflict areas, military training areas and munitions disposal sites [Davies, 1996; Detloff et al., 2012; Eitner and Tröster, 2018]. A number of risk management strategies exist [Novik et al., 2023]. However when UXO cannot be avoided or safely removed, *in-situ* explosive ordnance disposal (EOD) may be necessary. The favoured disposal method has historically been to use a high-order controlled detonation conducted by exploding a newer donor charge[1] mass placed adjacent to the munition for disposal [Cooper, 1996; Sayle et al., 2009; Albright, 2012; Aker et al., 2012; Cheong et al., 2020; Nowak et al., 2022]. This process is often referred to as *blast or blow-in-place* (BiP). These disposals produce acoustic pulses, which can make significant contributions to the soundscape over a wide area [Sertlek et al., 2019; Merchant et al., 2020; Robinson et al., 2022], and can have several adverse environmental consequences. These include the risk to marine fauna from exposure to the high amplitude sound levels produced [Yelverton et al., 1973; Ketten et al., 1993; NOAA, 2016; Dahl et al., 2020; Todd et al., 1996; Finneran et al., 2000; Danil and St. Leger, 2011; Sundermeyer et al., 2012; von Benda-Beckmann et al., 2015; Parsons et al., 2000; Salomons et al., 2021; Cottrell and Dupuy, 2021; Siebert et al., 2022; Robinson et al., 2022; Jenkins et al., 2022; Smith et al., 2022; Favretto-Cristini et al., 2022a, 2022b]. High-order detonations can be destructive to the seabed and create seismic signals detectable over great range [Binnerts et al., 2019], with relatively little known about the effect of the local acoustic and vibrational disturbance on benthic fauna on or close to the seabed [Hazelwood et al., 2018; Hawkins et al., 2021; Hazelwood and Macey, 2021]. In addition, both the long-term degradation of UXO, and its disposal, can also cause toxic chemical contamination [Strehse et al., 2017; Appel et al., 2018; Maser and Strehse, 2020, Schuster et al., 2021;

* Corresponding author.
E-mail address: p.a.lepper@lboro.ac.uk (P.A. Lepper).

[1] *Throughout this report the phrase 'charge' or 'charge mass' will be used to represent a measure of an amount of explosive material of comparable explosive power to the equivalent mass of TNT (TNT-eq). Note both historic, i.e. in the original UXO explosive material or through the addition of more modern explosive materials used in either a 'donor' or 'deflagration' charge are also stated as TNT eq. charge masses.*

https://doi.org/10.1016/j.marpolbul.2023.115965
Received 24 October 2023; Received in revised form 18 December 2023; Accepted 18 December 2023
Available online 13 January 2024

Table. 1
Description of *in-situ* WWII UXO based on diver surveys. ID column includes the Danish Navy name for the site for this operation, the explosive used to disarm the UXO ((HO) High-Order; (LO) Low-Order), the country of origin, and the presumed make and model of the UXO. [Annex A-F].

ID	Initial charge size (TNT eq.)	Condition
F-FOXTROT (HO) 18 m depth Mk 1–4 (Possibly a Mk6 mine, 430 kg)	~200 kg Amatol (estimated 60 % of the original 340 kg explosive charge remained)	Heavily encrusted with marine growth and the explosive section badly corroded with the filling exposed. ~450 mm burial.
G-GOLF (LO/HO) 19.5 m depth British possible Mk 6 mine	~344 kg Amatol (estimated at 80 % of original 430 kg)	Heavy marine growth and corrosion. The explosive charge section was open to the environment. ~100 mm burial. Fig. 1.
M-MIKE (HO) 18.5 m depth British Mk 1–4 mine	170 kg Amatol (estimated 50–60 % original 340 kg)	Covered in marine growth and very badly corroded. Estimated that the remaining explosive charge was approx. 50 % - 60 % of the original 340 kg charge weight exposed to environment. ~ 50 mm burial.
N-NOVEMBER (LO/HO) 17.5 m depth British Mk 1–4 mine	340 kg Amatol explosive main charge intact	Heavily covered in marine growth which obscured the overall mine case condition. Removal of some marine growth at the mid-position exposed the steel charge section, which looked to be in good condition. Burial ~ 150 mm.
J-JULIET (LO) 19.5 m depth British Mk 1–4 mine	340 kg Amatol original	Heavy marine growth. The end of the mechanism section was open to the environment and there were small areas of corrosion on the charge section, indicating that the explosive fill had been exposed to salt water, but there was no indication that the total charge had been reduced. Burial ~ 50 mm.
L-LIMA (LO) 17.5 m depth British Mk 4–6 mine	430 kg Amatol original	Heavily covered in marine growth. Its condition initially suggested that the explosive main charge had been protected from the environment ~ 100 mm burial. Fig. 2. Post detonation confirmed likely Mk 6.

Maser et al., 2023].

Impulsive sounds of very high-amplitude present challenges for effective mitigation, with potentially large exceedance areas for commonly used exposure thresholds [Finneran and Jenkins, 2012; Popper et al., 2014; NMFS, 2018; Southall et al., 2019]. Common mitigation strategies involve the use of spatial and temporal restrictions on the activity, visual and passive acoustic monitoring, and the introduction of additional noise of lower amplitude to create an aversive reaction by use of Acoustic Deterrent Devices (ADDs), and by use of small "scare" charges [JNCC, 2010; Merchant and Robinson, 2020]. Noise abatement technologies have also been employed including bubble curtains to attenuate the radiated sound [Loye and Arndt, 1948; Domenico, 1982; Schmidtke et al., 2009; Schmidtke, 2010; Schmidtke, 2012; Croci et al., 2014; Merchant and Robinson, 2020].

In recent years, there has been a focus on alternative methods of disposing of UXO [Koschinski, 2011; Koschinski and Kock, 2009; Koschinski and Kock, 2015] including the use of low-order techniques such as deflagration. In this method, which until recently has been more commonly used for military EOD operations, a small, shaped charge creates a plasma-like jet which penetrates the UXO casing and initiates a low-order combustion [Pedersen, 2002; Merchant and Robinson, 2020]. In general, ordnance is designed to be insensitive to mechanical and thermal impact, such as would occur from bullet or fragmentation impact. Thus, it is possible to penetrate UXO with a high velocity projectile and not cause an explosion or detonation. Low-order tools or disruptors are designed to transmit enough reaction energy to the UXO explosive charge mass so that the case ruptures, but not so much energy as to cause a full detonation *via* chain reaction due to over-pressure. One definition of "low-order is any explosive yield less than a full high-order" [Cooper, 1996; Pedersen, 2002]. With insufficient pressure to detonate, the explosive material may instead react with a rapid burn, termed deflagration (essentially, vigorous burning with the reaction occurring at sub-supersonic speeds). In the EOD community, it is taken to mean any process whereby a cased munition is caused to burn internally, but without complete detonation (no initialization of a shock wave). Low-order deflagration is a much less energetic process and underwater

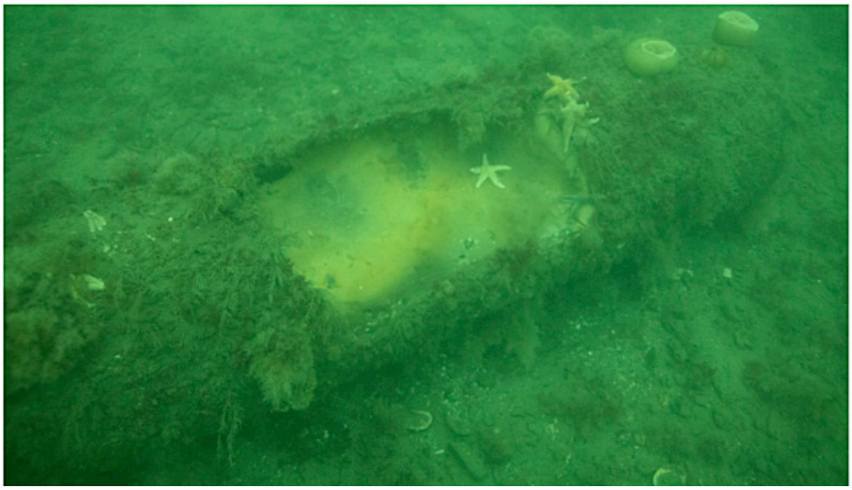

Fig. 1. GOLF – identified as *British Mk 1–4 mine (340 kg)*. Pre-clearance survey shows heavy marine growth and Amatol explosive exposed to the environment..

Fig. 2. LIMA – identified as *British Mk 6 mine (430 kg)*. Pre-clearance survey shows partial burial, but with the end plate exposed. Original explosive material was deemed to be fully intact.

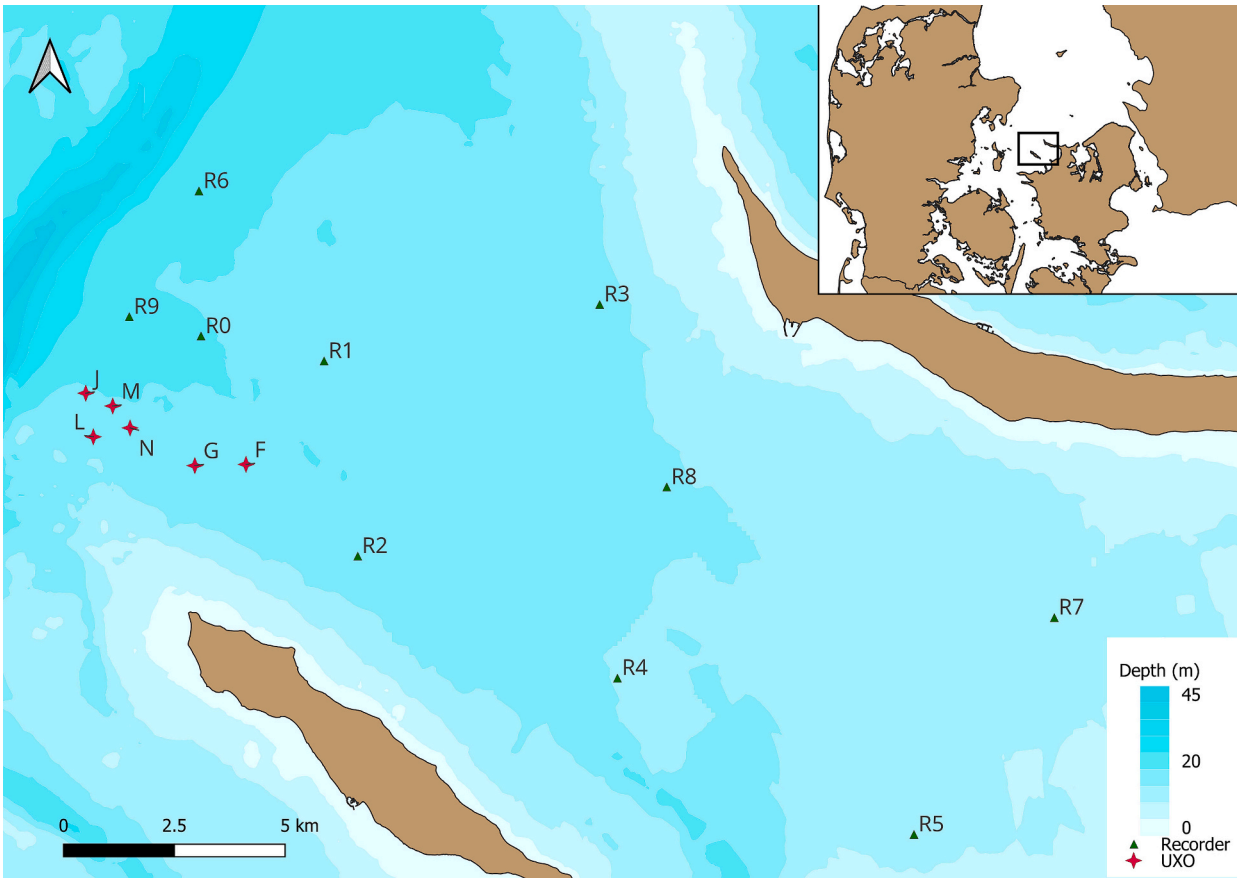

Fig. 3. Map of depth bathymetry across the trial site. Showing location of the UXO (red crosses) and static recorders (black triangles). For reference the NOVEMBER (N) UXO to recorder station R5 is approximately 25 km. (For interpretation of the references to colour in this figure legend, the reader is referred to the web version of this article.)

controlled experiments have shown that it has a much-reduced acoustic output with the peak sound pressure level and sound exposure level being around 20 dB lower for low-order deflagration compared to high-order detonation of similar charge sizes [Robinson et al., 2020].

The UXO for this study were WWII British sea mines located in the Great Belt in the Danish Straights. In total 8 EOD clearance events were carried out by the Royal Danish Navy on 6 UXO between 22nd-23rd January 2022 operating from Danish Navy vessel, Y311 Søløven. Of these mines two (identified as FOXTROT and MIKE) were cleared using a high-order methodology using 10 kg donor charge in a manner typical for traditional high-order EOD clearances. Two (JULIET and LIMA) were cleared using a low-order deflagration methodology and remaining two (GOLF and NOVEMBER) were initially cleared using low-order-order deflagration. The Danish Navy also then high-ordered the remainder

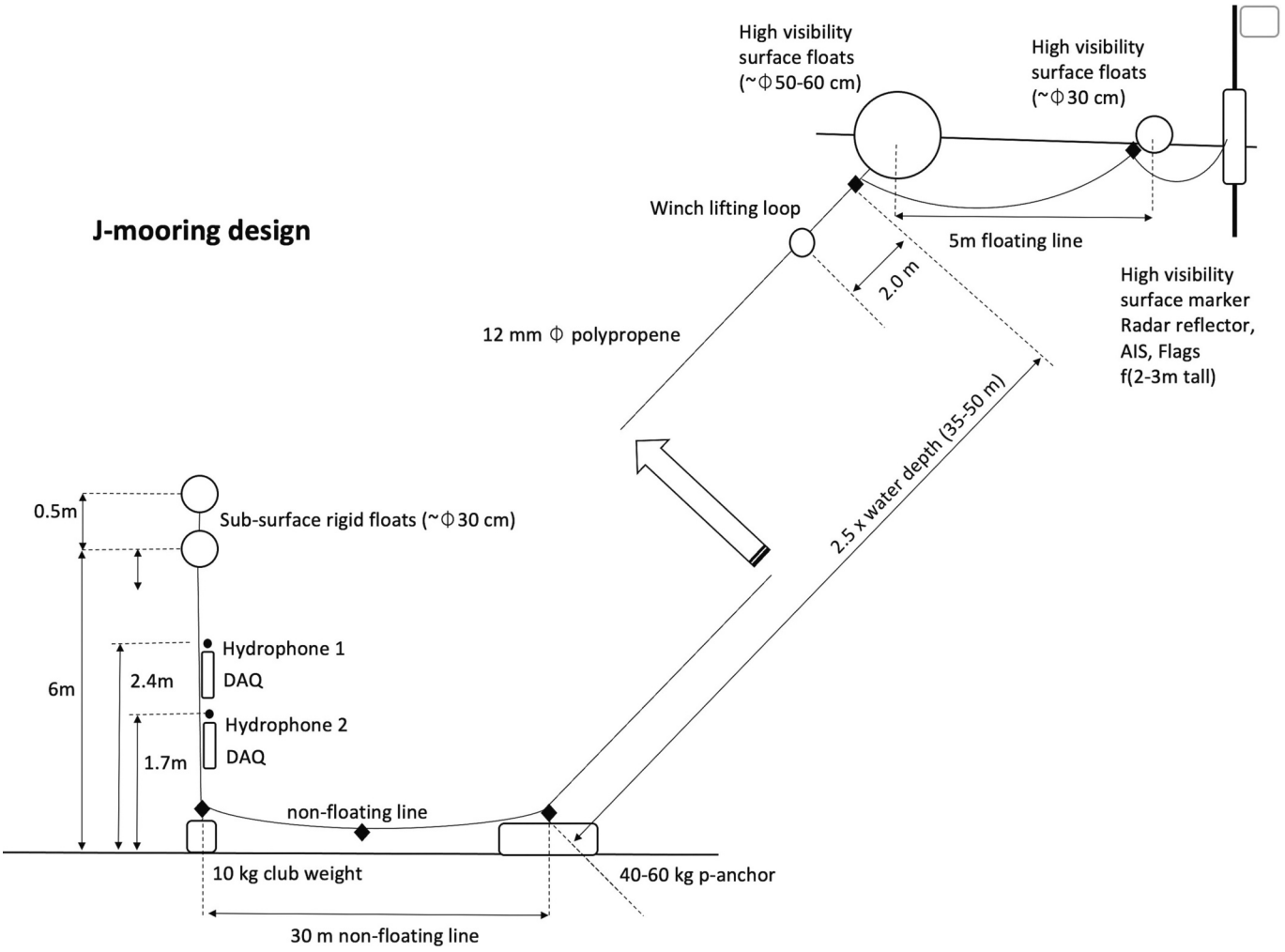

Fig. 4. `J-mooring design used on static recorder stations A0 – A9 in water depths 25 m – 12 m.

from the low-order of these two UXO. These latter two examples allowed acoustic measurement of both low-order deflagration and high-order methodologies from the exact same source positions and recorder ranges.

Details of the 6 UXO investigated in this trial are given in Table 1. and EOD assessment reports in supplementary material annex A-F. All had considerable marine growth sometimes making identification difficult and several were corroded. In the case of FOXTROT, GOLF, MIKE, and JULIET, the UXO charge was exposed to the environment and where possible estimates were made of the reduction of the bulk charge due to this exposure. EOD operators identified the explosive in each case as likely to be Amatol (main charge) with Tetryl Primers.

Other studies have reported the uncertainty in the acoustic output due to the unknown condition of the UXO, the degradation over time, partial burial, and potential for misidentification. This leads to uncertainty in the effective charge size for the UXO. For this study, the UXO were carefully identified by EOD professionals and Danish Navy experts, with photographic evidence recorded of the condition of each UXO, reducing the uncertainty surrounding the nature of the UXO under test. The measurements reported here on UXO disposals *in situ* follow on from measurements made under controlled conditions in a flooded quarry [Robinson et al., 2020]. This paper describes experimental work to compare the characteristics of the sound produced by deflagration with that of a traditional high-order detonation method for real UXO in an offshore environment (in the Danish Great Belt).

2. Experimental method

2.1. Locations and experimental configuration

Recordings were made using 10 seabed-mounted autonomous acoustic recorders deployed by the *RV Aurora*, operated by Aarhus University at a variety of ranges. These were closest of around 1.98 km to >22 km from the UXO's, the recorders being left in place for the duration of the operations. Fig. 3 shows the locations of the UXO and the acoustic recorders for the campaign. This array of hydrophones was primarily deployed to the east of the main UXO position due to the relatively uniform water depth ranging from around 15–20 m for most recorder ranges and up to 10–12 m at the most easterly recorders (R7, R5) with relatively smooth bathymetry across the area of interest. Note from Fig. 3 that the UXO were located just to the east of a deep-water channel (a major shipping lane) so care was taken to avoid deployment of recorders to the west of the UXO cluster.

Each measurement station (R0-R9) had one or two bottom mounted autonomous wideband recorder systems either deployed 1.7 m or 2.4 m from the seabed. Surface motion noise was decoupled from the recorders using a J-type mooring configuration as shown in Fig. 4.

Four types of water column wideband acoustic recorder types were deployed depending on location including 3× Soundtrap ST202HF, 9× Soundtrap ST300HF, 1× ST600, by Ocean Instruments (New Zealand) and 2× DSG-ST recorder by Loggerhead Instruments (United States). All recorders except 1× ST300HF (R5) and the ST600 (R4) were set to low

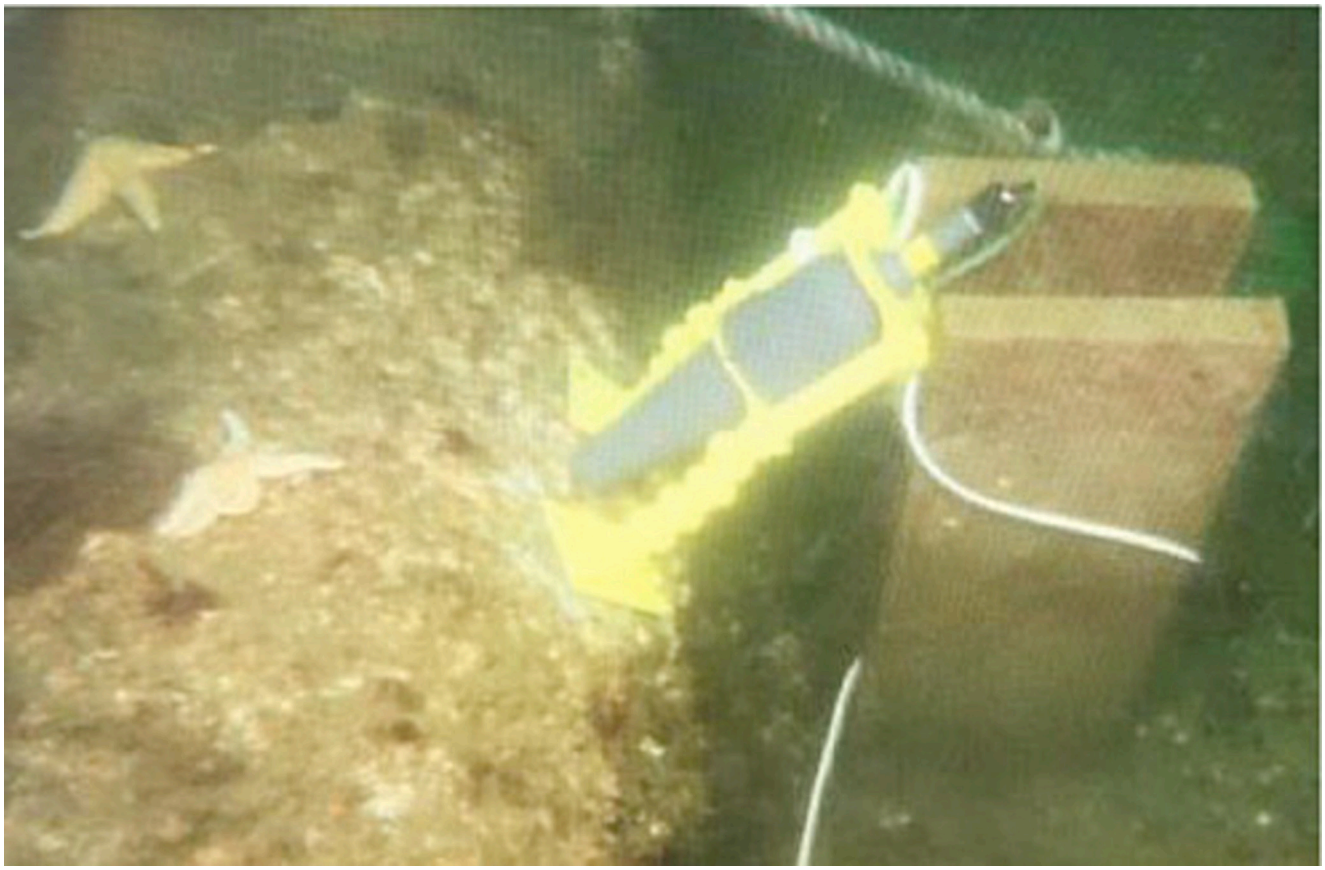

Fig. 5. Placement of a 250 g (Pluton) 'low-order' deflagration charge on the mine GOLF pre-low-order clearance.

sensitivity mode. A sample rate of 288 kHz used on all except the ST600 where the sample rate was 384 kHz.

In addition, two independent vertical arrays were also deployed from the side of the deployment vessel, see further details below.

Note that high bandwidth systems were used to allow best capture of the transient nature of the explosive events in the time domain. The sample rates used also allowed capture of any higher frequency components in the most sensitive hearing range of harbour porpoise (*Phocoena phocoena*) which is common in the Danish Straits. In addition, a commercial seabed vibration GPR1500 measurement system [Sercel, 2023] containing three axis accelerometer and hydrophone channel was deployed as part of the mooring R0. The system was resting on the seabed 5 m from the recorder up-line as shown in Fig. 4.

Acoustic measurements were also made from the *RV Aurora* which was repositioned for each of the clearance events with ranges 1.54 km - 6.08 km from the UXO. These positions were based on the combination with the static recorder array (R0-R9) and safety considerations requiring a blast exclusion zone. Measurements were made from the Aurora using two independent vertical hydrophone arrays. Array 1 consisted of 2 x Neptune Sonar T50 hydrophone positioned at 5 m & 10 m respectively from the surface, data was captured *via* a dedicated laptop with a eight channel Picoscope 4824 data acquisition unit, with sample rate ranging from 1.25 MHz – 2.5 MHz; array 2 was a bespoke four channels Soundtrap recorder fitted with 2 x HTI Type 96 hydrophone configured in low sensitivity (nom. Sens. -210 dB re 1 V/μPa) with sample rate of 384 kHz, the hydrophone elements were positioned at 5 m & 11 m respectively for the first two UXO disposal (FOXTROT & GOLF), positioned at 7.5 m & 15 m respectively for the remainder of the trial. In addition, sound velocity profiles were taken from the the Aurora using a Xylem Sontek Castaway CTD probe directly before and after each event.

All hydrophone systems were calibrated by NPL to IEC 60565–2:2019 standard and where possible calibration checks were undertaken using piston phone recordings made on each recorder system directly before and after deployment [IEC 60565-1, 2020; IEC 60565-2, 2019]. As far as possible, the measurement procedure followed the protocol defined by the UK Department for Business Energy and Industrial Strategy [BEIS, 2020], based on the procedures described in NPL Good Practice Guide 133 [Robinson et al., 2014] and ISO 18406 [ISO 18406, 2017]. The sample rates on all pressure sensor systems were sufficiently high enough to provide good representation of the waveform for assessment of peak pressure values [Meins et al., 2019].

Each UXO clearance was pre and post surveyed by Navy dive teams including video and photographic data. Sediment and water samples were taken in direct vicinity of the UXO at the seabed by divers. Dependant on safety clearance, chemical swabs of the sea surface were taken using ethylene & tetrafluoroethylene (ETFE) copolymer nets directly above the clearance event from a small dive boat. Water / sediment samples and surface swabs were then frozen for storage and later chemical analysis. Dinitrotoluene and trinitrotoluene content of the samples was determined by solvent extraction with analysis by high performance liquid chromatography with UV detector (HPLC-UV). The Danish Navy vessel Søløven also conducted a series of high-resolution sonar surveys both before and several months after clearance events to evaluate UXO clearance and seabed damage.

2.2. Unexploded ordnance disposal (EOD) methodologies

2.2.1. Low-order (deflagration)

The tool used was a PLUTON™ shaped charge manufactured by Alford Technologies [Patent WO 03/058155, 2003]. In the case of the Pluton a shaped charge of 250 g detonates causing instantaneous evaporation of a metallic cone, and this shaped charge punches a small hole (typically 10–20 mm diameter) through the outer UXO casing. The

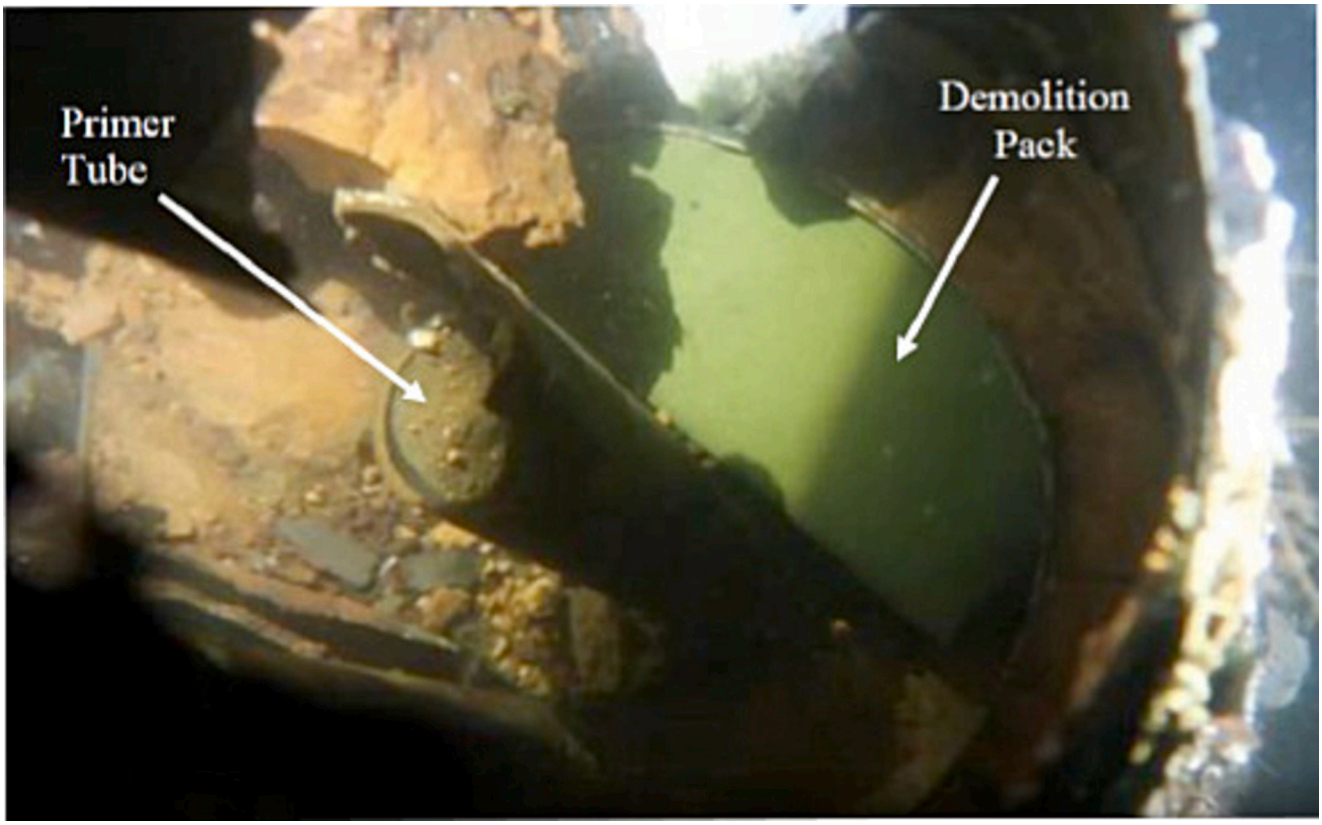

Fig. 6. Placement of a 10 kg 'high-order' donor charge on the mine GOLF pre- high-order clearance.

vapourised metallic cone material in the form of plasma like jet is injected into the bulk historic explosive material at around 5000° C initiating a slow (sub-supersonic speeds) burning deflagration process compared to the rapid (greater than supersonic speeds) detonation process as seen in a high-order event. This burning process can go on for several seconds and typically consuming a percentage of the explosive fill which generates gas from the decomposition of the explosive. In the case of a fully sealed system the accumulation of this gas can cause the pressure to rise in the UXO case causing it to burst at the weakest point before a full high-order detonation can occur. In these trials low-order deflagration methodology was tried on both sealed (fully intact) and unsealed UXO; for example, Fig. 5 shows placement of the Pluton charge on the UXO GOLF. Note in this case the bulk explosive material in GOLF was exposed to the environment as shown in Fig. 1. In contrast UXO LIMA (Fig. 2) was fully intact as well as partially buried.

2.2.2. *High-order (detonation)*

In these trials a modern high explosive charge size equivalent to 10 kg (TNT) is placed in the vicinity to the UXO by the dive team.

Fig. 6 shows an example a typical high-order donor demolition pack placed in the vicinity of UXO GOLF. This charge is detonated using a detonation line, intended to result in a near instantaneous additional detonation of the historic explosive material in the UXO. Typically, a high-order event would initiate a rapid combustion process at supersonic speeds and will result in the generation of a shock wave. Note that if the historic explosive material was to detonate at its full potential the equivalent total charge size is the historic charge + the modern donor charge (typically an extra 5–10 kg TNT equivalent).

3. Acoustic modelling of propagation

Source time domain waveforms were obtained using a modified Arons model using the time constants 2.2 & 8 s [Arons, 1954]. The model was applied at a distance of 10,000 times of the radius of the explosive, and then back propagated to get the waveform at source. From this waveform the source spectrum components across a bandwidth of 1 Hz to 2 kHz in steps of 1 Hz were then applied to range dependant propagation model RAM [Collins, 1993]. The time domain waveforms were then reconstructed by combining the individually range modelled frequency components to allow estimation of both $L_{p,pk}$ and SEL metrics at various range intervals. The seabed properties used in the propagation models were based on [Hamilton, 1980] given in Table 2. The modelling included a sound speed profile measured *in situ* and a typical on-site bathymetry profile are shown in Fig. 3. (See Fig. 7).

Table 2
Parameters used for propagation modelling.

Property	Water	Sediment Layer
Sound speed (ms^{-1})	1453	1652
Density (gcm^{-3})	1	1.772
Atten. (dB/λ)	[Skretting and Leroy, 1971]	0.83
layer thickness (m)	variable 10–20	Semi-infinite

State geological surveys data of Denmark and Greenland report the seabed in the area is mainly muddy sand [MARTA, 2023] with a relatively large sediment depth [Straume et al., 2019]. Due to lack of more details of the seabed properties, such as layered structures and their associated acoustic properties with which the shear wave could have been accounted for the seabed was treated as a simplified semi-infinite fluid with constant acoustic properties. There is some variation in bathymetry over the Sejerø Bight area where the UXO were cleared (see Fig. 3). Due to the wide spread of UXOs and recorders deployed, the bathymetry profile from UXO MIKE to recorder R7 was used for the modelling as the furthest from source. There was a small change in sound speed over depth, however, there is a decrease of water depth along the path from the UXO to the recorder as shown in Fig. 7. These simplification were then applied to a range dependant Parabolic

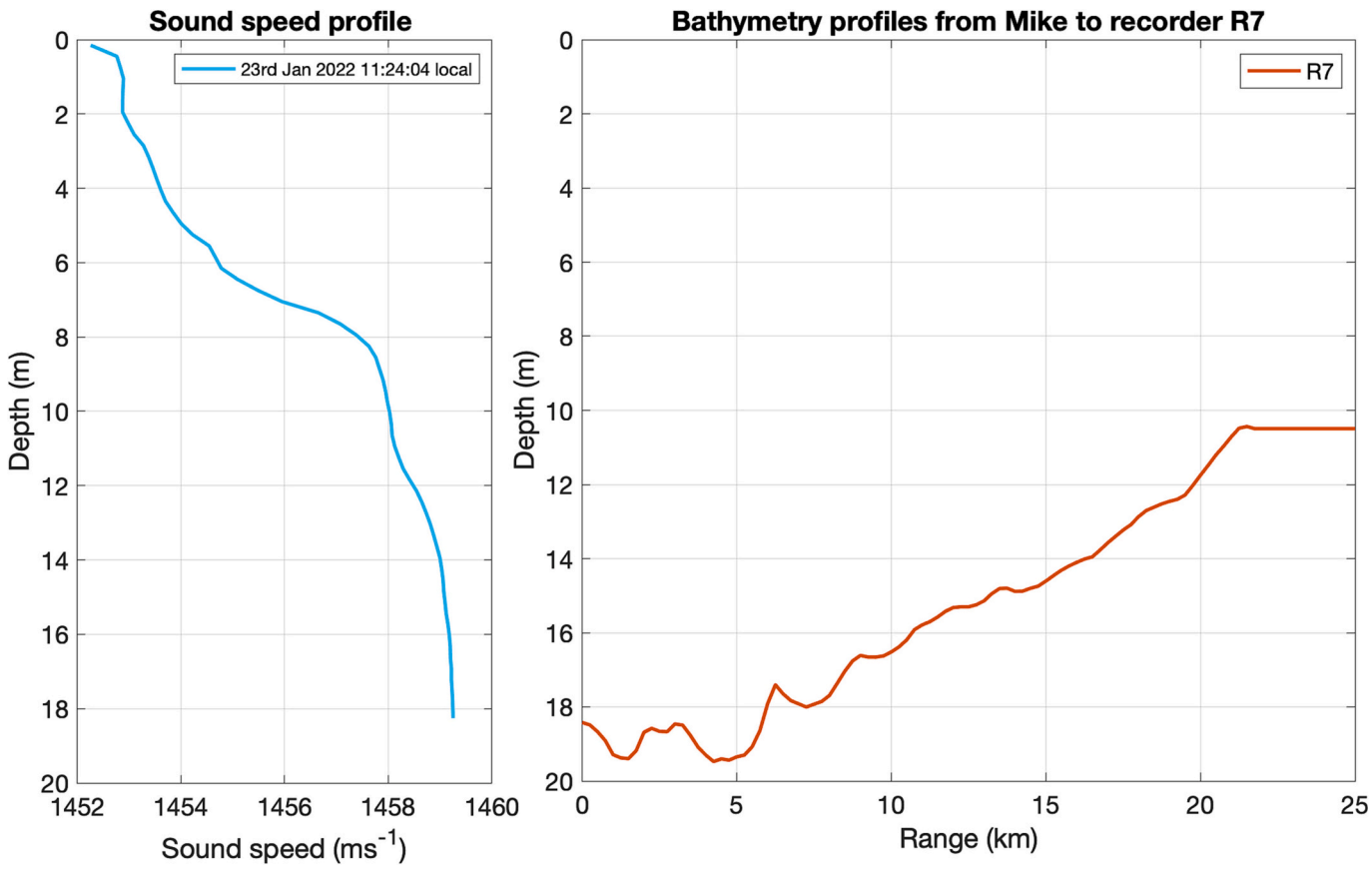

Fig. 7. Measured sound speed profile (left) and bathymetry profile between UXO MIKE and recorder R7.

Equation (RAM) propagation loss model.

The derived modelled received level *versus* range profiles for both SEL and $L_{p,pk}$ metrics combined with the original theoretical source characteristic spectrum [Arons, 1954] are shown as the modelled profiles in Figs. 12 & 13 for comparison with measured data of received level *versus* range in Section 4.3. The same methodology described above for deriving the broadband (1 Hz - 2 kHz) propagation loss profiles from the modelled time domain for each metric in isolation were fitted to measured received level data points to allow back propagation in estimation of the effective linear source level presented in Section 4.4. and impact range assessments Section 4.8.

Note that propagation loss profiles used in the back propagation for the effective linear source level presented in Section 4.4. and impact range assessments Section 4.9 were derived from the spectral content for a theoretical 430 kg source [Arons, 1954] to allow inclusion of as broad as possible spectrum particularly for higher frequencies. This was felt to be a conservative approach as these higher frequencies are likely to be of relevance to higher frequency animals such as harbour porpoise. However, it is acknowledged that these propagation loss profiles used were also limited by the modelling bandwidth of 2 kHz as described in Section 3. Measured data shown in the decidecade band analysis shows that the 2 kHz bandwidth used was sufficient to capture the energy contained in the −3 dB bandwidth of a typical high-order source at 3.1 km range. Despite this Fig. 14 does show above background energy levels at frequencies above 2 kHz particularly at shorter ranges but these often attenuated relatively quickly at longer ranges and their overall influence on the broadband time domain metrics considered was relatively minor.

4. Results

4.1. Summary of outcome of the EOD operations

All of the operations were deemed successful from an Explosive Ordnance Disposal (EOD) perspective. Table 3. summaries the post clearance analysis of the EOD operations.

Inspection was carried out by divers and sonar operations from the Navy vessel Søløven with 4 low-order clearances on GOLF-1, NOVEMBER-1 and JULIET and LIMA and 4 high-order operations FOXTROT, GOLF-2, MIKE and NOVEMBER-2. For all of the high-order events a 10 kg composite-B detonation pack was placed in direct contact with the mine. For the low-order clearances, a single Pluton deflagration (250 g) charge was used exterior to the main UXO shell.

In the case of the high-order events significant surface plumes and evidence of seabed cratering were observed with no mine fragments detectable post event. For the low-order events local damage occurred to the mines with splits and bursting of outer UXO shells, particularly when the UXO was initially intact, with much of the shell material remaining but with evidence of deflagration burning of UXO explosive material without high-order detonation. Shell material and explosives where typically within a few meters of the clearance site with no obvious seabed damage. No surface plumes were observed with the low-order events. None of the 4 low-order deflagration trials observed were considered to have undergone a deflagration to detonation transition (DDT) [Gupta et al., 2022].

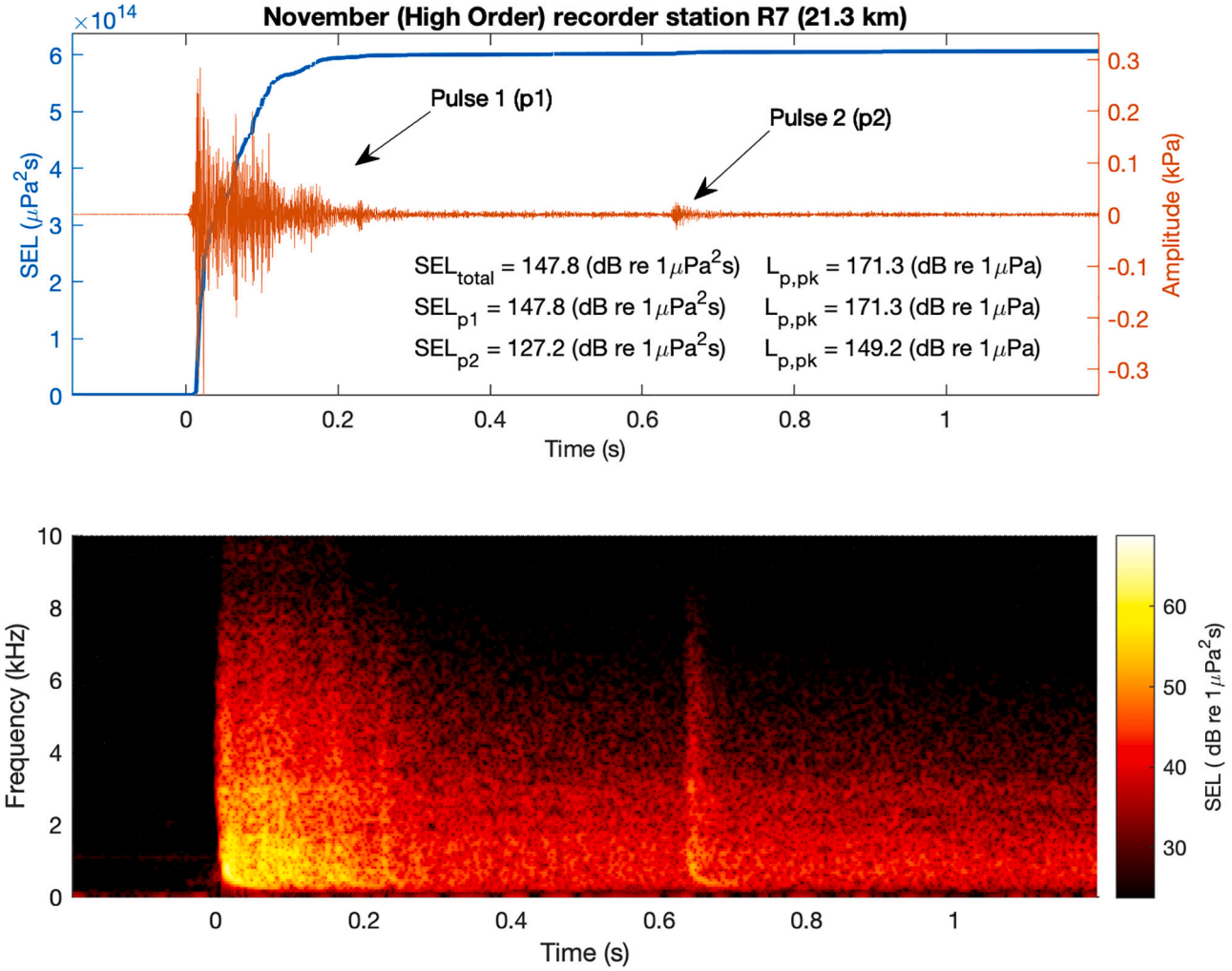

Fig. 8. High-Order: Upper panel shows the time domain plot of low-order event on UXO NOVEMBER at recorder station R7 at 21.3 km range (red trace-right hand vertical axis scale) superimposed on the cumulative energy SEL (blue trace – left hand vertical axis scale. The lower panel shows the equivalent short time frequency analysis. (For interpretation of the references to colour in this figure legend, the reader is referred to the web version of this article.)

4.2. Acoustic time-frequency analysis

The recorded data for the acoustic pulses were analysed and two acoustic amplitude metrics were calculated: peak sound pressure in Pa (sometimes referred to as the zero-to-peak sound pressure) and its level ($L_{p,pk}$) in dB re 1 μPa; and the sound exposure level (SEL) in dB re 1 μPa^{2}s calculated both as a broadband value and in decidecade bands (sometimes termed one third octave bands calculated using base 10 [ISO 18405, 2017]) and using short time Fourier transforms [Mitra, 2001]. The focus was on these metrics because they are key to the calculation of exposure for certain classes of marine mammals and fish [Southall et al., 2019; NMFS, 2018; Popper et al., 2014]. The definitions of these terms were adopted from ISO 18405 [ISO 18405, 2017], with the calculations on the acoustic pulse following the procedure described in the protocol [BEIS, 2020].

Fig. 8 shows a data from a high-order clearance of the NOVEMBER mine as recorded at station R7 at a range of 21.3 km. Spectral analysis shown in Figs. 8 & 9 were generated using a sample rate of 288 kHz a 4096-point FFT window with a Hann window and a 4000-point overlap. SEL total values integrated over 1.4 s window. Pulse 1 and Pulse 2 SEL values were integrated over 0.7 s respectively. The time domain plot shown in the upper panel shows a strong initial pulse arrival of peak level ($L_{p,pk}$) of around 171 dB re 1 μPa around 0.25 kPa and total SEL value of 143.8 dB re 1 μPa^{2}s integrated across the full 1.4 s shown in the figure. By comparison Fig. 9 shows the initial low-order event that took place on NOVEMBER with an estimated charge size of 340 kg + 0.25 kg (Pluton) charge at the same distance. In the latter case the levels peak level ($L_{p,pk}$) of 151.2 dB re 1 μPa and total SEL value of 125.3 dB re 1 μPa^{2}s again integrated across the full 1.4 s window shown. The low-order case shows significant reduction in levels of around 20 dB for peak level and 18 dB for SEL. These reductions in levels were seen consistently across all the events analysed between high and low-order and at various ranges. Both high and low-order signal parameters were generally consistent with previous observations of explosive detonations in shallow water of varying charge sizes [Gaspin et al., 1979; Chapman, 1985; Chapman, 1988; Hannay and Chapman, 1999; Soloway and Dahl, 2014; Robinson et al., 2020; Salomons et al., 2021; Robinson et al., 2022; Favretto-Cristini et al., 2022a, 2022b].

The high-order events consistently showed a secondary pulse (arriving at around 0.65 s after the main signal arrival in the example shown in Fig. 8) which is not present in the case of the low-order events. The delay of this signal varied from around 0.6 to 0.8 s across the four high-order events recorded. Bubble pulsation intervals of around 0.8 s have been previously reported by Gitterman for high order detonations in the Dead Sea but for much larger charge sizes (500, 2060 & 5000 kg) [Gitterman, 2009]. The delays seen here were however was not consistent with for example the first bubble pulse expansion and collapse for a 22 kg TNT – eq charge mass at 20 m depth expected to be

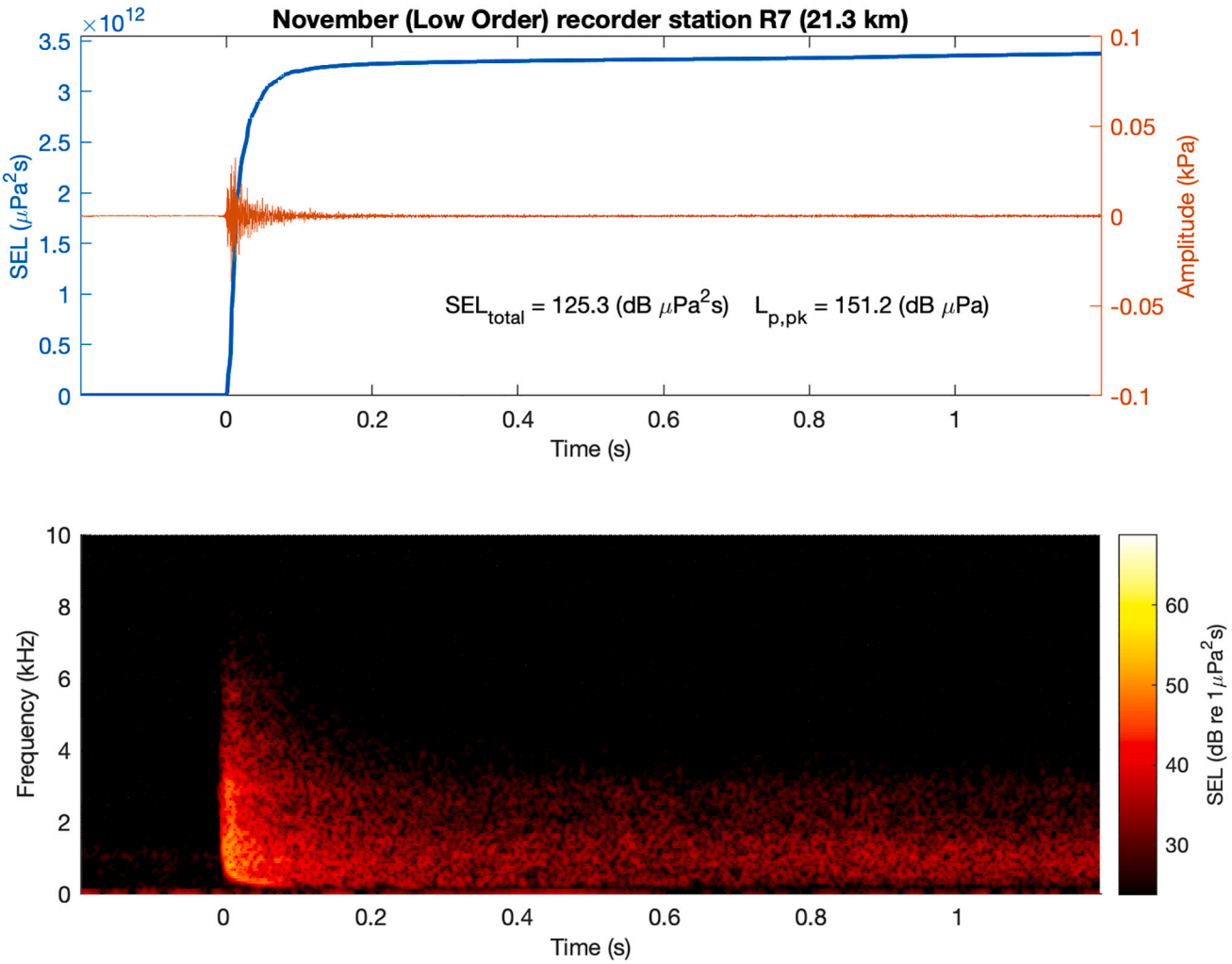

Fig. 9. Low-Order: Upper panel shows the time domain plot of low-order event on UXO NOVEMBER at recorder station R7 at 21.3 km range (red trace-right hand vertical axis scale) superimposed on the cumulative energy SEL (blue trace – left hand vertical axis scale. The lower panel shows the equivalent short time frequency analysis. (For interpretation of the references to colour in this figure legend, the reader is referred to the web version of this article.)

around 0.38 s, and 1.03 s for 440 kg charge including a 10 kg donor charge. [Cole, 1948; Arons, 1970]. Using these models for the likely actual charge mass based on the acoustic levels, the first bubble would be expected sooner than observed in the acoustic data and may be buried in the complex multipath arrival seen in the signal at this larger range. Mis-estimation of the actual charge size could account for discrepancy in this delayed bubble signal. Variation in this delay is also possible due to complex interactions with both the seabed and the surface compared to a deeper-water non-seabed detonation [Favretto-Cristini et al., 2022a]. The delay is also inconsistent with an echo arrival from any bathymetric features. Analysis of video data taken from the Aurora showed that the time delays showed some correlation with the point that the surface water plume begins to collapse *i.e.* the moment that the peak of the plume is reached (Fig. 10.). Time $t = 0$ from video data was taken as the arrival of the initial shock wave at the surface. Note these plumes were only seen with the high-order clearances which projected a large column of water many metres into the air. Analysis of video data from high-order events also often showed a secondary darker coloured plume assumed to be associated with mixing of the water with sediment. The sequence of the evolution of the surface plumes were generally consistent with previous researchers observations of underwater high-order detonations for example observations of 500, 2060 & 5000 kg charge masses detonated at round 70 m depth in approximately 265 m water depth in the Dead Sea [Gitterman, 2009].

Many of the events showed evidence of potential sediment-borne waves with some variation in amplitude and arrival time. These often-lower frequency acoustic arrivals were sometimes observed arriving as a precursor before the main water column arrivals as typically shown in Figs. 8 & 9 and were variable in timing with changes in range. Evidence of seabed surface vibrational waves were also evident and are also discussed further in Section 4.6.

Fig. 10 shows the evolution of this water plume cycle observed on the high-order NOVEMBER clearance. Analysis of both the initial and secondary pulses seen in all the high-order events showed that although they have similar spectral distributions with the relative difference in the wide band amplitude between the pulses, the secondary signal made only a very minor contribution to the overall energy of the signal. In the NOVEMBER event (Fig. 8) this contribution contributed <0.04 dB to the total SEL and therefore was generally negligible although interesting in origin. However, although comparatively small compared to the main signal (SEL_{p1}) in the case of comparison of the SEL metric with broad-band impact thresholds the overall signal SEL_{total} including the second pulse is used in this analysis. This effect was not observed on the low-order clearances.

The lower panels in Figs. 8 and 9 show the short time Fourier transform spectrogram for both the high and low-order events. Both show the sharp transient rise time and arrival initially with higher frequency components arriving first with detectable energy levels up to 30

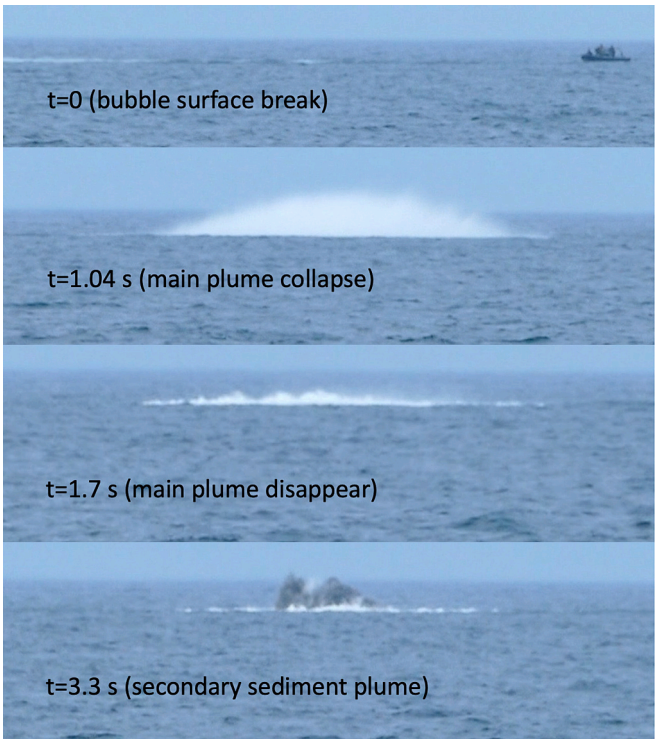

Fig. 10. The high-order clearance water plume as seen from the Aurora at a range of 1.54 km. Note the upper panel also shows the small dive team zodiac for scale.

kHz. A down sweep of the slower lower frequency arrivals can then be seen containing much of the energy of the signal. An extended tail to the main signal is then seen consistent with a complex multipath arrival in this relatively shallow water and at this range from the source. It should be noted that the low-order clearances although significantly lower in level compared to the high-order events still demonstrate similar time-spectral characteristics. This is consistent with the notion that the shaped charge used in this low-order deflagration method is effectively also a high-order detonation but at a significantly lower TNT eq. charge mass of 250 g and therefore related amplitude.

Fig. 11 shows decidecade band analysis of the received signal at a range of 21.3 km for both the high and low-order NOVEMBER clearance events. The spectral content levels of both are similar with most of the energy in the bands from 200 Hz to around 13 kHz at this range, with very little energy above this upper frequency. The frequency of the peak energy levels in both cases is around the 1 kHz band with band levels >20 dB higher for the high-order compared to the low-order events.

4.3. Amplitude level versus range

Data shown in Section 4.2 has focused on high and low-order event characteristics at the longer ranges recorded to allow direct comparison of both high and low-order signals characteristics over similar distances. The significantly higher levels seen from the high-order events can prove challenging to measure with standard commercially available recording systems at shorter ranges. In these trials, data from of all the high-order events at ranges of <18 km recorded at the static moorings suffered from some form of clipping, making analysis of the spectral content of these events more difficult. However, data from the lower sensitivity higher dynamic range system deployed from the Aurora allowed capture of good quality data for all events down to ranges of a few km. Figs. 12 and 13 show analysis for all of the events for peak pressure $L_{p,pk}$ and total SEL *versus* ranges for all the available data with the maximum measured peak sound pressure level of 209 dB re 1μPa and SEL of 191.4 dB re $1\mu Pa^2s$ at a range of around 1.54 km for the high-order NOVEMBER clearance.

Direct comparison of both the high and lower order clearances of NOVEMBER at a range of around 19.8 km, showed high-order SEL levels of 150.2 dB re $1\mu Pa^2s$ whereas the low-order clearance of the same target were 17 dB lower at 133.2 dB re $1\mu Pa^2s$. Similarly, the peak level values were 173.3 dB and 159.2 dB re 1μPa respectively from high and low-order showing a 14.1 dB reduction. Note that the NOVEMBER high-order clearance was of the remainder from the preceding low-order event (of 340.25 kg including the deflagration charge) with a residual combined charge estimated to be around 44 kg including the 10 kg donor charge. Taking the combined historic and donor or deflagration clearance equivalent charge masses into account, the low-order deflagration clearance was around 17 dB and 14 dB lower in acoustic levels for both the SEL and $L_{p,pk}$ metrics although the effective charge mass being cleared was nearly eight times larger than the associated high-order clearance. These data also show that the high-order SEL levels of 133 dB re $1\mu Pa^2s$ and peak levels of 159 dB re 1μPa were close to what might be expected from the 10 kg donor charge mass on its own. This suggests in this data that a majority of acoustic energy detected from this high-order event was due to the donor and not the donor + remaining historic charge. By comparison the high-order clearance of MIKE gave peak levels of 197.9 dB re 1μPa and SEL levels of 176.7 dB re $1\mu Pa^2s$ at ranges of around 6 km. These levels were around 4 dB below the theoretical modelled levels for a 340 kg detonation at the same range but at a level around 7 dB above the modelled 10 kg on its own suggesting in this case some of the historic charge may have contributed to the overall noise level. Comparison with a low-order event on GOLF demonstrated a 17 dB lower SEL level and >21 dB lower peak level for these high and low-order clearances respectively at a similar range.

Figs. 12 and 13 both show consistently lower amplitude levels between the high and low-order methodologies for both metrics with a consistent reduction of between 15 and 20 dB at all the ranges measured. Comparison with the modelled data based on 250 g deflagration charge shows a reasonable correlation for the low-order events levels consistent with contribution from the deflagration charge (250 g) only with a good fit to the measured $L_{p,pk}$ metric out to 25 km with similar reasonable agreement for the SEL metric but with the model slightly overestimating values at ranges >15 km. This was consistent with data seen in previous comparison trials of high and low-order conducted in a quarry in 2019 [Robinson et al., 2020.]. Similarly, most of the high-order events show a reasonable correlation with a contribution expected from the 10 kg donor charge used plus some contribution from the UXO charge. Particularly at lower ranges the SEL model appears to give slightly higher results than seen in some of the measured data. Similar effects were noted from analysis of 54 historic UXO clearances in the North Sea [Robinson et al., 2022] and in measurements of UXO in Danish waters [Salomons et al., 2021] and Dutch waters [von Benda-Beckmann et al., 2015]. It has been hypothesised that the misalignment between the model and measured data may be because most empirically based models such as Weston's [Weston, 1960] assume a mid-water detonation, whilst almost all UXO clearances take place at the seabed [von Benda-Beckmann et al., 2015; Robinson et al., 2022]. In this case significant amounts of energy are likely absorbed by the seabed and the resultant seabed disruption (Section 4.7). Soloway and Dahl [2014] also reported lower measured levels than model predictions for non-seabed detonations in similar shallow water environments to the cases described above. Other hypothesis suggested for the over prediction of some modelled data include energy lost due to shielding by cavitation and to surface blowout as seen in Fig. 10. [von Benda-Beckmann et al., 2015]. Salomons *et al*, applied an empirically derived adjustment to compensate for the effect for measured high-order events.

In this current study the high-order amplitude data is in general close in level to what might be expected from the 10 kg donor on its own. These observations are generally consistent with most of the 54 measured historic UXO events analysed by Robinson et al. in the North

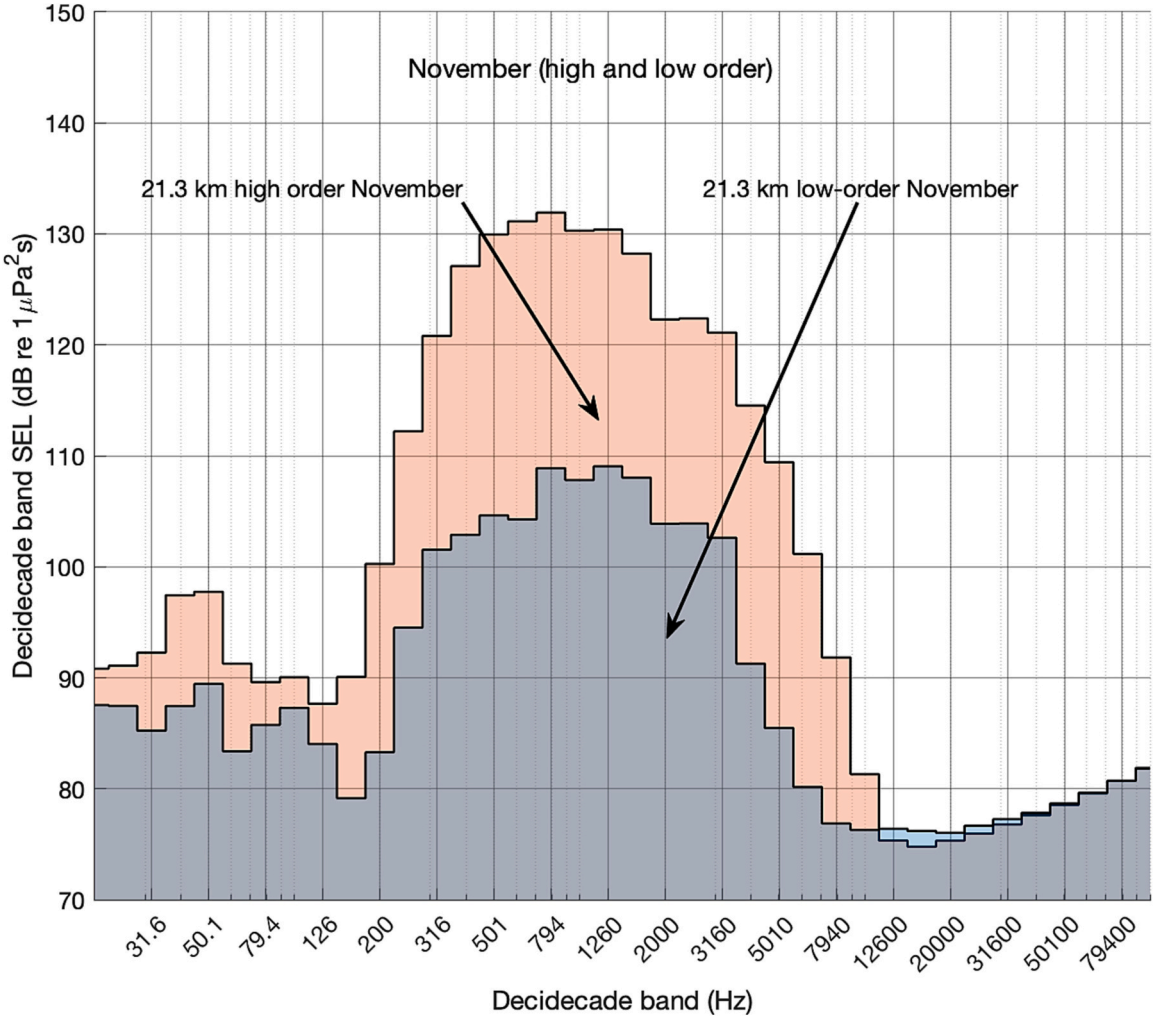

Fig. 11. Comparison of decidecade band levels for long range (21.3 km) high and low-order clearances on mine NOVEMBER. Analysis window 1.2 s.

Sea [Robinson et al., 2022]. This implies that observed levels in both these trials were not as high as what could be expected if the donor plus the historic explosive material was to explode at its full potential. Robinson *et al* did also show examples of events where much higher levels were measured in line with a significant contribution from both the donor and the historic charge and the potential for much higher levels will always exist from both high and low-order methodologies if the historic explosives do detonate either partially or fully. The range of the measured data bounded by a suitable propagation loss curve (derived using methodologies described in Section 3) for both metrics is given in Figs. 12 and 13 as shaded areas. Table 4. gives a summary of the wideband data recorded on the lower element of the T15 vertical array deployed from the Aurora.

Fig. 14 shows the variation in spectral content *versus* range for the low-order clearance of LIMA. At shorter ranges (3.6–6 km) the spectral distribution is relatively flat in the range of a 30 Hz to around 8 kHz, with peak band level at around 50 Hz. However, low frequency components <300 Hz have largely been attenuated to levels comparable to background noise at range of around 22 km. This results in a shifting the peak band level into the region 700–1200 Hz, with a corresponding reduction in overall amplitude. It can also be seen that at the shorter ranges (3.3 km) that signal levels are detectable in the frequency bands between 20 and 100 kHz. These higher frequency components however had largely disappeared at ranges >6 km. Both effects are consistent with what might be expected from propagation in a shallow and upward sloping environment due to low frequency mode-stripping and higher frequency absorption effects. In the latter case, at ranges much greater 12 km, levels above 20 kHz are signal levels comparable with background levels.

4.4. Source level

Monopole equivalent Source Levels were estimated for both SEL and $L_{p,pk}$ metrics. These were obtained for each of the metrics using the broadband propagation loss models outlined in Section 3. These were then fitted through each of the measured metric data points and back propagated to 1 m. Fig. 15a shows an example of the curve fit for high-order clearance of mine MIKE and Fig. 15b low-order clearance on GOLF. Each data point was back propagated allowing estimation of a distribution of potential source level estimates for each event, see Table 5 which gives the midpoint and upper and lower limits of source level estimates obtained. Note this back propagation to short ranges in determining the source level assumes linear propagation and the estimated source levels may only be used for far-field predictions at ranges greater than several water depths. At very close ranges, the presence of the shock wave from the explosion will modify the acoustic field.

Table 5 shows the estimates for both SEL and $L_{p,pk}$ for each of the eight clearance events. The high-order events had an estimated source levels in range 243–246 dB μPa²s-m for SEL and 255–266 dB μPa-m for $L_{p,pk}$. Source Levels were estimated using best fit estimates of a high-level signal transmission loss profile (430 kg) through each of the measured data. Fig. 15a, shows the high-order clearance data for MIKE

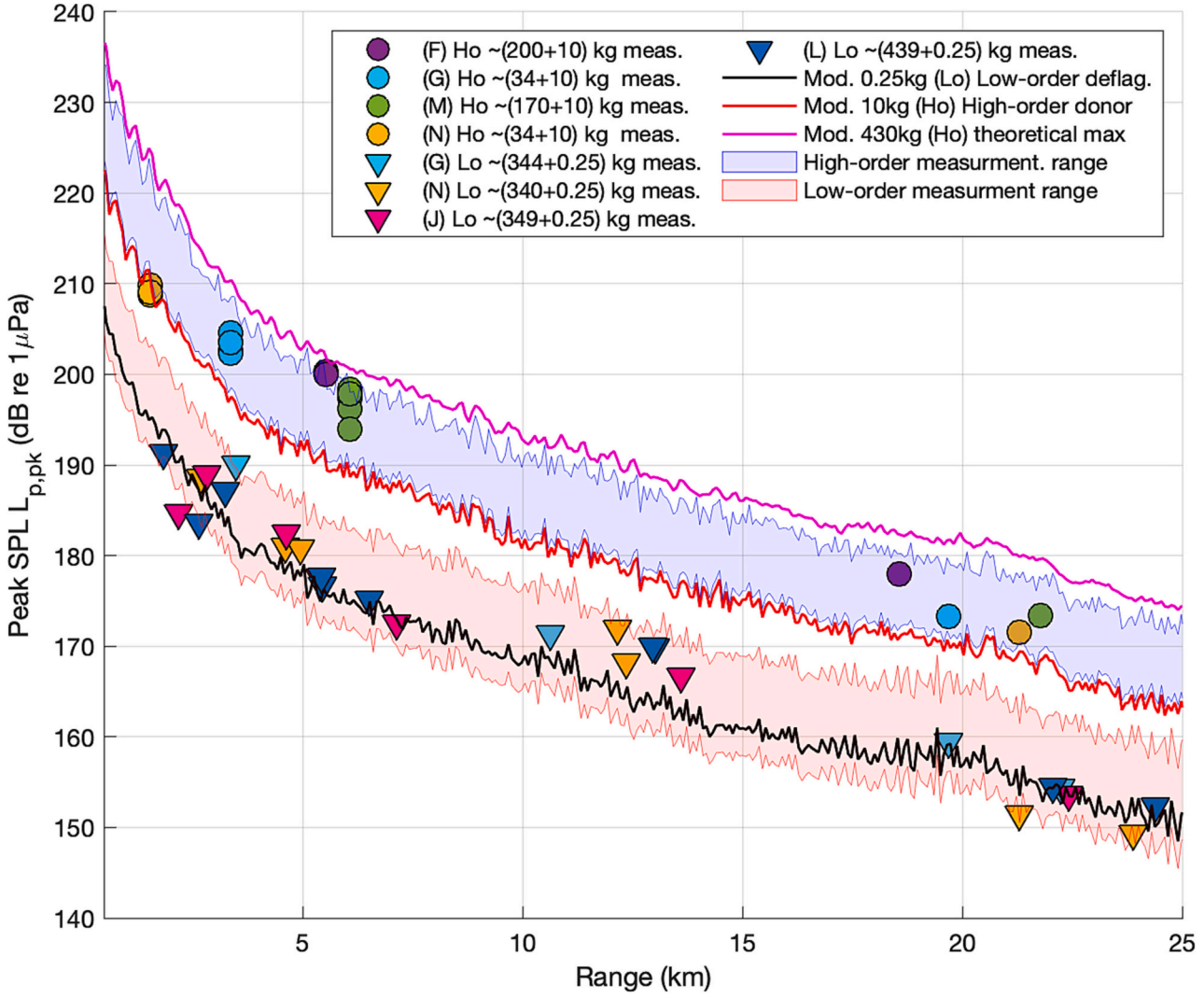

Fig. 12. Peak sound pressure level ($L_{p,pk}$)for all eight events *versus* range. Circles show high-order (HO) events and triangles for low-order (LO). Filled markers are directly measured. Solid lines are modelled data for the 250 g Pluton charge on its own, a 10 kg donor charge on its own and a theoretical maximum of 430 kg for a Mk 6 mine. Shaded areas represent the range of measured high and low-order data fitted to a modelled propagation loss profile for this area.

with a mid-range value of 263.3 dB μPa-m (± 2.1 dB) and a potential overall maximum $L_{p,pk}$ equivalent linear source level of around 265 dB μPa-m seen on the FOXTROT clearance.

Using 250 g propagation loss profile estimates of the low-order events showed source levels in range 217–219 dB μPa^2s-m for SEL and 240–245 dB μPa-m for $L_{p,pk}$ with the maximum of around 248 dB μPa-m for $L_{p,pk}$ seen on the clearance of GOLF (shown in Fig. 15b). All of the low-order source levels estimates were remarkably stable with values of around 225 dB μPa^2s-m and 242 dB μPa-m for SEL and $L_{p,pk}$ respectively. By comparison the high-order events showed a wider divergence with clearances of FOXTROT and MIKE being typically as much as 5–6 dB higher $L_{p,pk}$ levels than the GOLF and NOVEMBER high-order clearances. This is most likely reflective of the higher historic charge presence observed in FOXTROT and MIKE clearances. This effect is still present in the SEL metric although less pronounced. Comparison of all the high-order clearances give levels of 244.3 ± 1.25 dB μPa-m and 262 ± 5 dB μPa^2s-m for SEL and $L_{p,pk}$ respectively.

Comparison of the two low-order and then high-order clearances at similar ranges on GOLF and NOVEMBER show source level estimates around 15 dB lower $L_{p,pk}$ and 15–17 dB lower SEL than the measured following high-order events at the same range. It should be noted however that both the GOLF and NOVEMBER high-order event was of a relatively smaller charge residual (left over from the associated low-order clearance) historic charge sizes of around 44 kg including the high-order donor charge of 10 kg, see Table 5. This can be compared with the FOXTROT high-order clearance with a potential charge size of around 440 kg with a $L_{p,pk}$ source level of around 265 dB, approximately 24 dB higher in level than the low-order clearance of LIMA for a similar sized MK 6 weapon. Comparison of the of all measured high-order *versus* low-order source level estimates give estimates around 19 dB lower for low-order compared to high-order for both SEL and $L_{p,pk}$. Note that these relative reductions in measured levels and estimated source levels correspond to linear scaling factors of around 9 x quieter for $L_{p,pk}$ and 80 times quieter for SEL for low compared to high-order operations for these clearances.

The variation between the modelled equivalent TNT charge masses based on the acoustic levels (shown in column 4 Table 5.) compared to the estimated actual physical UXO charge mass (shown in column 5 Table 5.) may be due to a variety of causes. These can include uncertainty in the models used in shallow water discussed by various authors [von Benda-Beckmann et al., 2015; Soloway and Dahl, 2014; Favretto-Cristini et al., 2022a, 2022b; Robinson et al., 2022], uncertainty in the remaining UXO charge mass, typically estimated by visual inspection and uncertainty in the UXO's explosive material viability due to chemical degradation over time and potential long-term exposure to the marine environment. All these effects or combination of them can

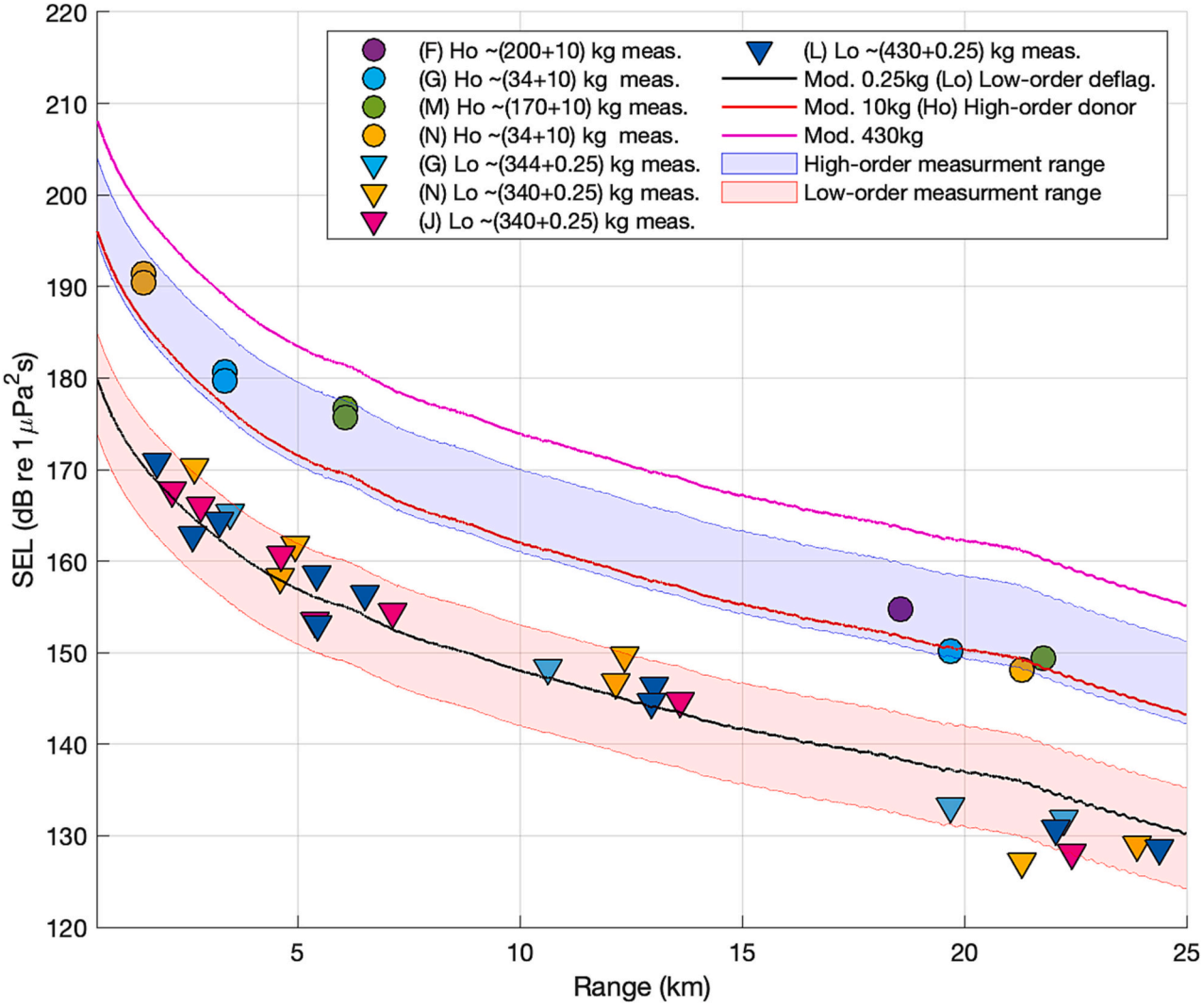

Fig. 13. SEL pressure for all eight events *versus* range. Circles show high-order (HO) events and triangles for low-order (LO). Filled markers are directly measured. Solid lines are modelled data for the 250 g Pluton charge on its own, a 10 kg donor charge on its own and a theoretical maximum of 430 kg. Shaded areas represent the range of measured high and low-order data fitted to a modelled propagation loss profile for this area.

account for effective lower levels often seen from historic UXO charge masses clearance events compared to that of the equivalent underwater explosive model predictions. In the case of the modern explosive components used in these operations the lower uncertainties in both the amount of explosive material present and its explosive viability means a much higher level of predictability of the contribution of these components to the total acoustic amplitude levels observed.

4.5. Seabed vibration

Measurements were made using the Sercel seabed system described in Section 2.1 at recorder station R0. The R0 station was kept in the same position throughout all the trials with distances to the sources ranging from a minimum of 2.54 km for (MIKE – a high-order)) to a maximum of 3.25 km for (LIMA a low-order). Additional acoustic pressure field date was available from the R0 hydrophone system. Fig. 16a shows an example of spectral data for the signal arrival from the NOVEMBER high-order event (upper panel) and NOVEMBER low-order event (lower panel). Both events were recorded at the same range of 2.55 km.

Note the broadband arrival seen at times <3 s are the acoustic arrivals through the water column. However, in the case of the high-order event at around 6 s after the initial acoustic arrival a low frequency component with dominant frequencies of around 5–6 Hz can be seen which corresponds to seabed vibration, in this case the vertical component. These vibration components are not easily detected in the spectral analysis in the low-order event. Similar responses are seen in the horizontal acceleration axis in the direction of sound propagation with detectable vibration signal visible in the high-order events and significantly lower levels on the low-order events.

Figs. 16b show a significance difference in low frequency vertical acceleration of the seabed instrument at a range of 2.55 km for both high-order and a low-order event compared with background levels. In the case of the high-order event relatively high levels exist across a spectrum from a few Hz to 100 Hz. In some cases, with levels >80 dB above background, with the highest levels in bands between 3 and 5 Hz. By comparison the low-order event has vertical acceleration values on average 30–40 dB lower than the high-order with a peak energy in the decidecade band again centred around 3 Hz.

Note absolute values for acceleration here are based on the manufacturers calibration and attempts were made to allow the recording system to rest uniformly on the seabed. Although this is its manufacturer standard operational mode, the systems actual direct coupling to the seabed is unknown and therefore a degree of uncertainty in the absolute values exists. However, the relative levels stated above can be seen as

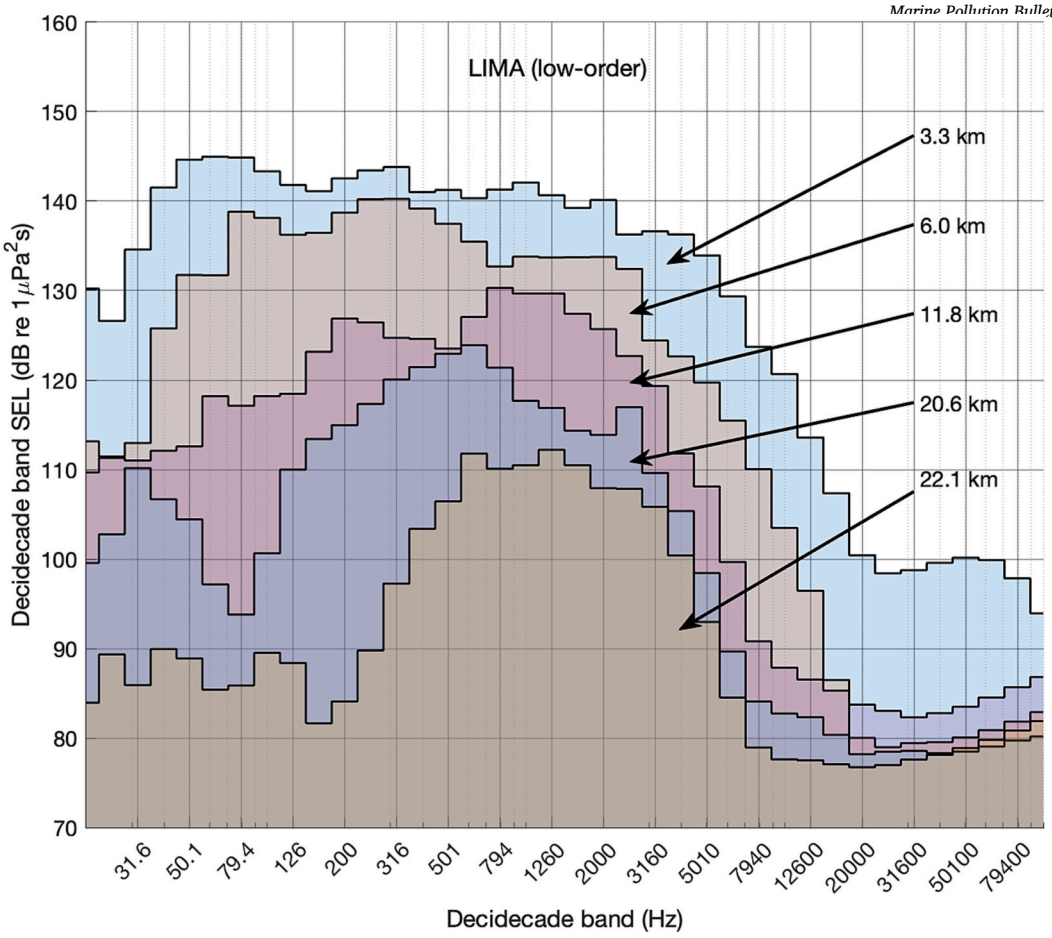

Fig. 14. Decidecade band levels *versus* range for low-order clearance 'LIMA'. Analysis window 1.2 s.

Table 3
Sequential summary of eight clearance events across the six UXO {Annex A-F: Supplementary material}.

Clearance event	Disposal method	Post clearance survey summary based on diver side scan sonar and visual inspection. (source [Annex A-F])
F-FOXTROT [~200 kg Amatol	High-order 10 kg donor charge	High-order detonation successful. Significant surface plume observed. No obvious mine remains. Generation of crater ~ 4 m diameter 1 m deep.
G-GOLF- 1 [~344 kg Amatol]	Low-order 250 g Pluton deflag. Charge	Deflagration successful, mine had not detonated. Estimated <10 % original explosive remained. This explosive residue was scattered in and around the remaining mine-carcass. No obvious seabed damage.
G-GOLF- 2 [~34 kg Amatol]	High-order 10 kg donor charge	High-order detonation successful. Significant surface plume observed. No obvious mine remains. Seabed cratering observed.
M-MIKE [~170 kg Amatol]	High-order 10 kg donor charge	High-order detonation successful. Significant surface plume observed. No obvious mine remains. Generation of crater ~ 6.4 m diameter
N-NOVEMBER — 1 [~340 kg Amatol]	Low-order 250 g Pluton deflag. Charge	Deflagration successful, mine had not detonated. Estimated <10 % original explosive remained. This explosive residue was scattered in and around the remaining mine-carcass. Over pressure split of mine casing. No obvious seabed damage..
N-NOVEMBER — 2 [~34 kg Amatol]	High-order 10 kg donor charge	High-order detonation successful. Significant surface plume observed. No obvious mine remains reported.
J-JULIET [~340 kg Amatol]	Low-order 250 g Pluton deflag. Charge	Deflagration successful, mine had not detonated. Deflagration had still burst opened the main explosive section. Explosive residue was scattered in a similar manner to that witnessed in the other mines.
L-LIMA [~430 kg Amatol]	Low-order 250 g Pluton deflag. Charge	Deflagration successful, mine had not detonated. The mine charge case had almost been cut in half with much of the Amatol burned or ejected during the process of deflagration.

Table 4
SEL and SPL ($L_{p,pk}$) levels measured at a water depth of 10 m from a single element of the T15 vertical array.

ID	Received level SEL (dB 1μPa²s)	Received level $L_{p,pk}$ (dB 1μPa)	Range (km)
GOLF (LO)	165.7 dB	191.6 dB	3.5 km
GOLF (HO)	179.7 dB	203.5 dB	3.4 km
MIKE (HO)	175.7 dB	197.5 dB	6.1 km
NOVEMBER (LO)	171.3 dB	190.6 dB	2.7 km
NOVEMBER (HO)	190.4 dB	209.0 dB	1.5 km
JULIET (LO)	168.4 dB	188.0 dB	2.2 km
LIMA (LO)	171.5 dB	192.2 dB	1.8 km

useful indication of the ratio of difference of effects seen at the seabed.

4.6. Seabed damage

The Danish Navy conducted clearance analysis of the seabed before and after each of the clearances using both diver inspection and diver scan sonar surveys. Fig. 17 shows a pre-survey of two mines conducted in June 2021 by the Danish Navy. In this case, pre-detonation, both mines can be seen proud of the seabed and no obvious cratering or scour in the area.

Fig. 18 shows typical post clearance side scan images for the same two high-order clearance events, FOXTROT and MIKE, in both cases

a

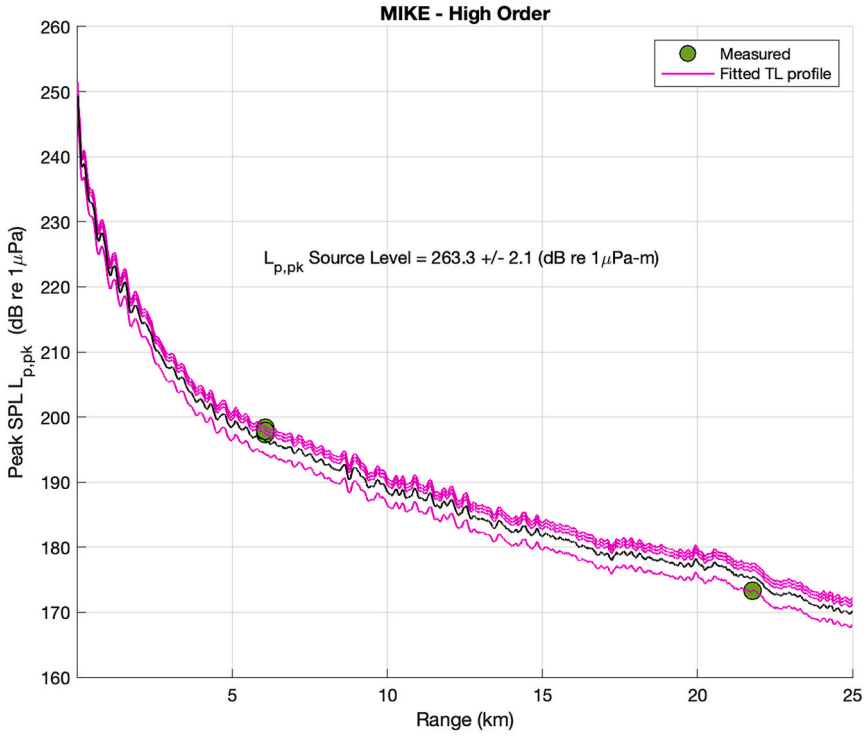

b

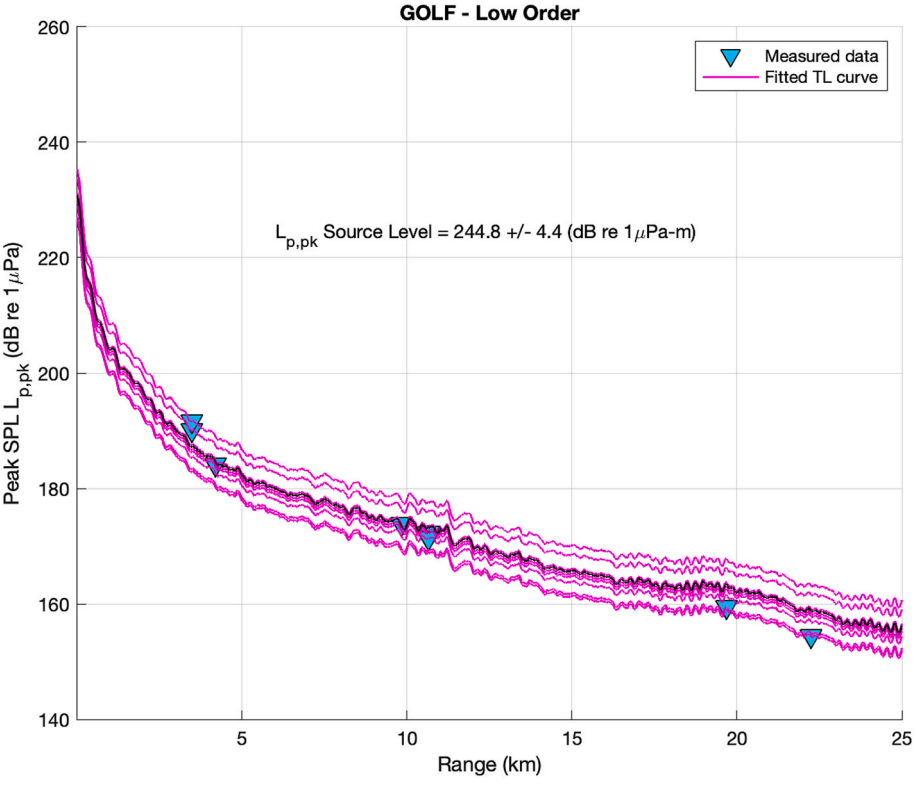

(caption on next page)

Fig. 15. a Propagation loss curve fit estimate *versus* range for high-order event on mine MIKE. Broadband propagation curve based on a 430 kg high-order detonation back propagated from measured data to an estimated equivalent linear source level. Purple solid lines are fitted transmission loss profile to individual measured data points. Black solid line midpoint received level profile based on all the fitted transmission loss profiles.
b. Propagation loss curve fit estimate *versus* range for low-order event on mine GOLF. Broadband propagation curve based on a 250 g low-order detonation back propagated from measured data to an estimated equivalent linear source level. Purple solid lines are fitted transmission loss profile to individual measured data points. Black solid line midpoint received level profile based on all the fitted transmission loss profiles. (For interpretation of the references to colour in this figure legend, the reader is referred to the web version of this article.)

Table 5
Zero-peak ($L_{p,pk}$) and SEL source level estimate for each event.

CLEARNCE ID	Measured equivalent linear Source Level estimate SEL -dB (μPa^2s-m)	Measured equivalent linear Source Level estimate $L_{p,pk}$-dB (μPa-m)	Measured acoustic values equivalent TNT -eq charge size using a linear SEL model [Arons, 1954] (kg)	Estimated Actual charge size (kg)
FOXTROT (HO)	244.9 dB (±0.0 dB)	265.4 dB (±2.1 dB)	22 kg	~200 kg +10 kg
GOLF (HO)	243.4 dB (±2.0 dB)	260.0 (±0.8 dB)	16 kg	~34 kg +10 kg
MIKE (HO)	245.9 dB (±3.0 dB)	263.3 dB (±2.1 dB)	28 kg	~170 kg +10 kg
NOVEMBER (HO)	243.8 dB (±3.1 dB)	255.5 dB (±3.8 dB)	17 kg	~34 kg +10 kg
GOLF (LO)	225.6 dB (±4.2 dB)	244.8 dB (±4.4 dB)	0.29 kg	~344 kg +0.25 kg
NOVEMBER (LO)	226.5 dB (±3.8 dB)	241.3 dB (±5.6 dB)	0.36 kg	~340 kg +0.25 kg
JULIET (LO)	224.0 dB (±4.3 dB)	240.4 dB (±6.3 dB)	0.21 kg	~340 kg +0.25 kg
LIMA (LO)	225.0 dB (±3.2 dB)	241.8 dB (±4.8 dB)	0.26 kg	~430 kg +0.25 kg

craters can be seen with diameters 4.3 m and 6.4 m respectively. Both craters were estimated to be 1 m - 3 m in depth. It is clear in the case of the high-order clearances that much of historic explosive material and the metallic casing has largely disappeared resulting in development of considerable craters in the seabed where the UXO had been. An assumption often historically made with high-order events that all the UXO material (metallic casing, explosives, and associated systems) have been fully consumed by the detonation process with minimal environmental contamination. Its unclear from the currents study if this is a valid assumption and warrants further investigation.

By comparison during low-order events once the smaller shaped charge penetrates the outer metallic casing the explosive material is either fully or partially consumed in the deflagration burning process. If the casing is intact this can lead to an over pressure and often result in a splitting open of the casing with minimum seabed disturbance. Fig. 19 shows example images taken post clearance by divers on two low-order events LIMA (upper image) and NOVEMBER (lower image). Note in both cases the casing has split open due to overpressure but did not result in a high-order detonation (deflagration to detonation transition DDT). The lower image shows the deflagration charge penetration point and minor damage due to over pressure. There was also evidence of consumption of the historic explosive through the deflagration process [Annex A-F]. Remnants of both the casing and potential explosive material are typically located within a few metres of the original UXO location with no obvious damage to the seabed.

Fig. 20 shows a multibeam survey of the high-order FOXTROT clearance site conducted by the Danish Navy in October 2022, nine months after the January 2022 clearance event discussed above. This still shows the evidence of the seabed cratering seen in Fig. 18 but also wide-ranging disturbance of the seabed out to around a 30 m diameter [Pers. Comms, Danish Navy].

4.7. Chemical residue analysis

Chemical sample analyses indicate no evidence for a surface slick of explosive residues post clearance. Concentrations of dinitrotoluenes and trinitrotoluene in sediment were variable, with evidence of existing contamination around all UXO examined, mostly <10 mg/kg but up to 2450 mg/kg of 2,4,6-trinitrotoluene (TNT) at the apparently intact mine JULIET. Low-order clearance may result in elevations in chemical residues, for example sediment concentrations of TNT at mine LIMA were 9.69 mg/kg before and 39,900 mg/kg after clearance. The samples were not replicated, and these results are considered preliminary and tentative although they are broadly consistent with the findings of [Maser et al. 2023] from a parallel contemporaneous study of explosive residues around mines MIKE and GOLF.

4.8. Noise exposure – Impact ranges

Estimates of the distance from source for avoidance of Temporary Threshold Shift (TTS) and Permanent Threshold Shift (PTS) for both high and low-order methodologies were made. Measured level data (Figs. 12 and 13) were combined with both SEL and $L_{p,pk}$ propagation loss profiles (propagation loss *versus* range) for the furthest R5 recorder station to estimate SEL and $L_{p,pk}$ Received Levels *versus* range for the low-order LIMA and high-order MIKE clearances. The measured SEL data was scaled dependant on calculated variation in the SEL metric received level for each of the functional cetacean hearing groups, Low Frequency (LF), High Frequency (HF), Very High Frequency (VHF) and Pinniped in Water (PW) based on calculation of the SEL metric before and after application of each of the weighted frequency functions to the broadband measured signal at relatively short ranges (MIKE 6 km & LIMA 1.8 km).

The SEL propagation loss profiles were then fitted through each of these weighting adjusted data points. From these profiles the potential variation in distance from the source required to allow avoidance of both PTS and TTS individual impact thresholds for each of the functional hearing response groups based on Southall et al., 2019 was estimated. The lower to upper limits shown in Tables 6 & 7 represent the estimate of lowest to greatest distances from source to generate levels below the impact thresholds based on the profile fits through each of the measured data points. An identical process was carried out for the $L_{p,pk}$ metric using unweighted $L_{p,pk}$ data points and the derived $L_{p,pk}$ metric propagation loss profile.

Table 6 shows the potential range of distance from the source that may be required to allow avoidance of a PTS type impact for each based functional hearing group. Similarly, Table 7 shows the data estimates for avoidance of TTS impact thresholds in these cases.

5. Conclusion

The reported measurements and additional modelling efforts in this study represent the first time that a comparison has been made in an offshore environment between high-order disposal and low-order deflagration EOD methodologies of UXO. In total eight clearance events were carried out by Danish Navy UXO clearance experts in

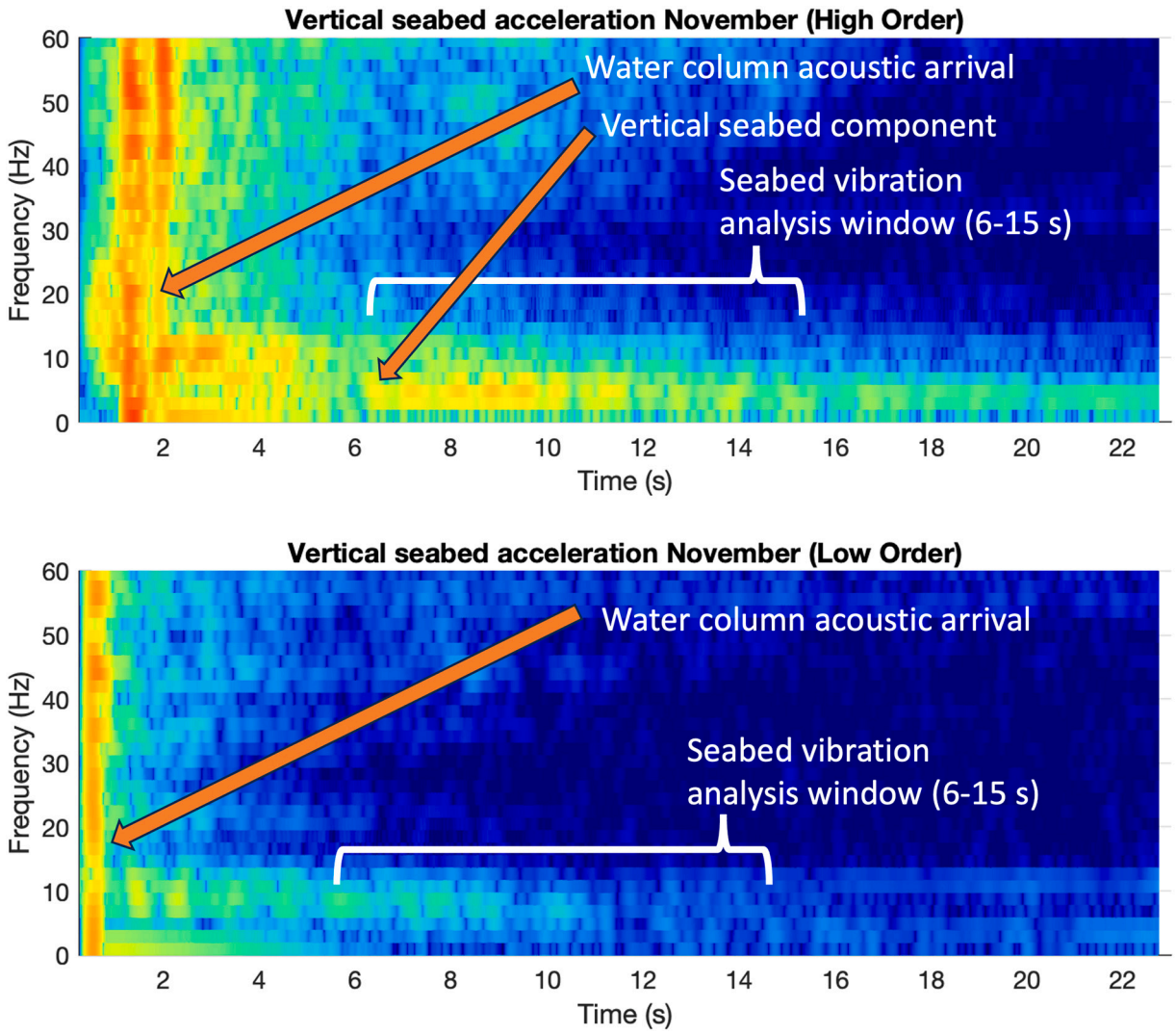

Fig. 16a. Spectral plot of acoustic and seabed vertical acceleration. The upper plot shows the high-order and lower panel the low-order event on the same target (NOVEMBER) both at a range of 2.55 km. Analysis in both cases was short time frequency analysis using MATLAB [Sample rate = 1 kHz, Hann window 512), overlap length = 511, FFT length = 512].

Danish waters in January 2022 of six British WWII sea mines of original charge size ranging from 340 kg – 430 kg. These were cleared using combinations of both high-order (detonation) and low-order (deflagration) clearance EOD techniques. In water column acoustic measurements were made for all events over ranges from <1 km to >22 km. In addition, a seabed vibration sensor was deployed at ranges from 2.5 to 3.5 km. Pre and post-clearance surveys were carried out using diver held scan sonar and visual diver inspection to assess EOD operations as well as potential seabed effects such as cratering. In addition, chemical analysis of event residues at the sea surface and in sediments were conducted.

The high-order methodologies used involved the detonation of a 10 kg (TNT equivalent) donor charge with the intent to initiate detonation of the typically larger historic UXO charge. The low-order deflagration methodology used a shaped charge technology of equivalent charge size around 0.25 kg intended to initiate a deflagration (slow burning) process rather than the detonation process seen in the high-order events. Typical acoustic pressure field measured data showed for both the high and low-order events significant acoustic levels were present out to ranges >20 km. These levels particularly for high-order events at shorter ranges represent some of the loudest man-made noise sources typically encountered in our oceans and waterways with estimated equivalent SEL linear source levels for high-order clearance events of around 244 dB re 1μPa^{2}s-m^2 and zero-to-peak linear source levels ($L_{p,pk}$) of >260 dB 1μPa-m. By comparison the low-order deflagration events were typically around 15 dB to 20 dB lower in amplitudes for both SEL and $L_{p,pk}$ metrics at all of the measured ranges. Acoustic levels for the low-order events were comparable with levels recorded from low-order deflagration clearance made in a quarry using surrogate modern explosive shells made by Robinson et al., 2020 in 2019. The acoustic levels associated with the low-order deflagration, although lower in level than high-order clearances do however still represent significant noise sources with estimated equivalent linear source levels comparable to that of marine piling operations [Ainslie et al., 2012; Robinson et al., 2012; Lippert et al., 2016; Martin and Barclay, 2019].

Data from this current trial also show evidence of similarities in observed slight discrepancies between measurements and predictions from modelled results. Similar discrepancies having been observed in measured and modelled data from most of 54 high-order UXO EOD events analysed by [Robinson et al., 2022] across two windfarm projects in the North Sea. This is particularly evident in data summarised in Fig. 21 for measured data from the current measurements for high-order events. These consistently showed slightly higher level than might be expected from the donor detonation on its own but none of the events generated levels as high as might be expected from the combination of the donor and the full UXO historic charge. This suggests some

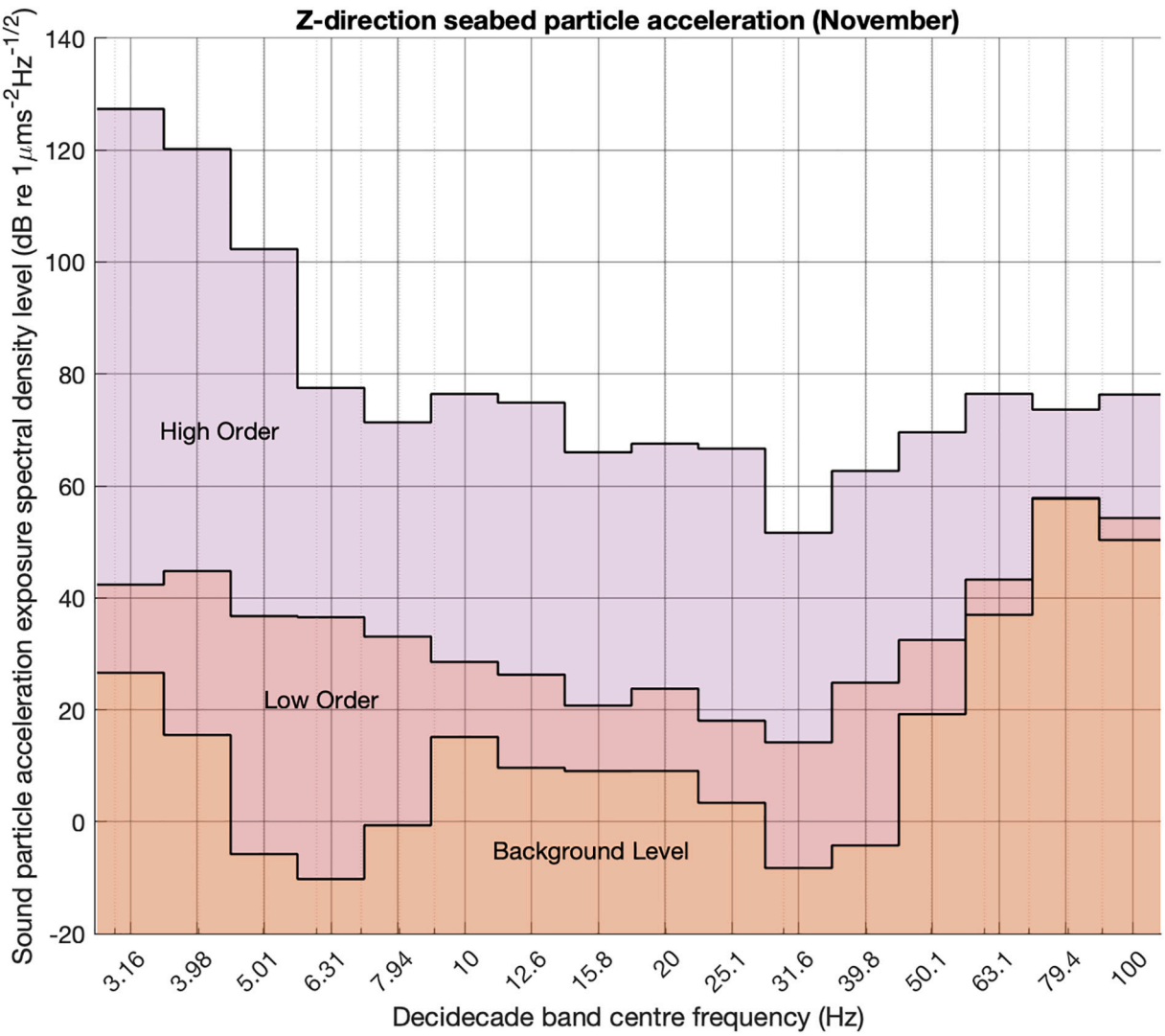

Fig. 16b. Decidecade spectral band analysis spectral of the vertical seabed acceleration for time period 6–15 s starting 6 s after the water column acoustic arrival as shown in Fig. 16a. The figure shows the high-order and the low-order event on the same target (NOVEMBER) both at a range of 2.55 km as well as background levels.

uncertainty in how much of the UXO historic charge actually detonates and/or is consumed as originally intended during high-order clearance process. This observation is supported by the data shown in Table 5, comparing estimated charge size based from measured acoustic levels with the reported historic UXO size of the weapon, where there is usually a significant reduction in the estimated equivalent TNT amount based on the observed acoustic levels compared to the actual weapon size for the high-order events.

Robinson et al., 2022 and others have discussed the potential for some contribution to the tendency of many explosive source acoustic models to slightly overestimate acoustic levels compared with measured data from real UXO being due to effects on detonation of the seabed. One possibility is that many of these models have been derived from empirical data collected from mid water detonations, whereas effect of the seabed absorbing a significant amount of the explosive and related acoustic could account for some of this discrepancy. In addition, observations so far from both the Great Belt and North Sea measurements suggest many real UXO, although not all, if high-ordered do not generate levels at the full potential of the original historic explosive charge. However, the minimum levels observed are in line with at least what would be expected from a donor charge on its own.

Comparison of data for both measured and modelled data from the low-order events in this trial also given in Fig. 21 and Table 5 show remarkably good agreement between predicted and measured levels as well as consistency between these events using similar modelling approaches to that of the high-order events. This aligns with the post clearance observations of these UXO's where the weapon is typically broken / split open, and a proportion of the historic explosive appears to be consumed *via* a deflagration process without any additional detonation of the historic charge.

Note that the modelled Received Level profiles for both the SEL and $L_{p,pk}$ metrics shown in comparison to broadband measured data, Figs. 12 and 13 were derived from the theoretical spectral content for source model [Arons, 1954] combined with a typical propagation loss profile in the direction of the R7 recorder station out to a range of 25 km and band limited from 1 Hz – 2 kHz (discussed in Section 3) for each of the metrics. The same loss profiles were then used in the back propagation from measured data points for the effective linear source level presented in Section 4.4 and fitted to measured data for the impact range assessments Section 4.8. In the case of frequency weighting factors used in the impact analysis used in Section 4.8 these were also derived using short range broadband measured signals to include as broad a frequency spectrum as possible in combination with broadband (> 100 kHz) measured data. There is however, the potential due to the use of the band limited (1 Hz – 2 kHz) propagation loss profiles to slightly overestimate frequency components >2 kHz due to not modelling the attenuation effects on

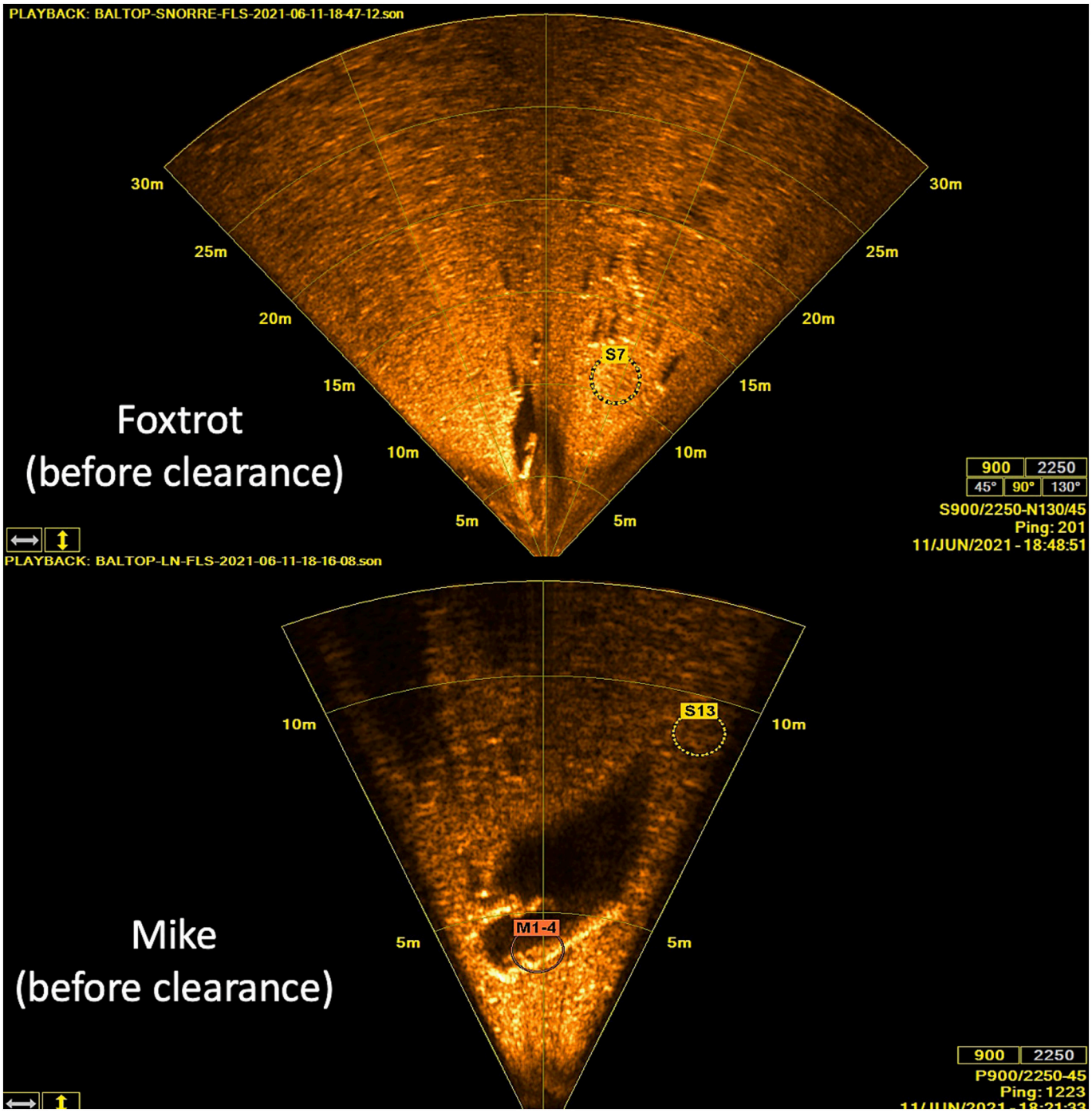

Fig. 17. Pre-clearance UXO diver sonar scan surveys of UXO's FOXTROT & MIKE conducted in June 2021. The upper image is from FOXTROT sonar scan image in 18.4 m water depth, sensor heading 106° with a + 3.1° pitch angle and MIKE in 18.1 m water depth on heading 95° and − 7° pitch.

these higher frequencies. Analysis of the >2 kHz signal contribution to the overall broadband metric values was however found to be generally insignificant. Similarly, comparison of source spectrum for both broadband measured and band-limited modelled data showed relatively good agreement. Due to this and particularly in the case of the SEL_{VHF} metric the band limited SEL propagation loss profiles used in the impact range assessment were felt to be a more conservative approximation for propagation loss for the most relevant frequencies to this analysis.

Conversely the non-inclusion of sub-surface sediment layers, interface wave and shear wave propagation effects in the propagation models used here may account for some discrepancies seen at low and ultra-low frequencies, in comparison with the measured data. Favretto-Cristini *et al* report the observation and importance of consideration of both seismic and acoustic wave propagation mechanisms to both water column and seabed paths as well as the propagation of interference type waves such as Stoneley-Scholte waves and shear wave propagation in sediment layers for explosive events particularly in shallow water environments [Favretto-Cristini et al., 2022a, 2022b]. In the current case the models used did tend to underestimate the water column acoustic content slightly at lower frequencies which may be due to some of these not considered propagation mechanisms described by Favretto-Cristini et al. However, as with the high frequency components, the overall contribution of these components to the general broadband metrics considered here were relatively small and the models and model

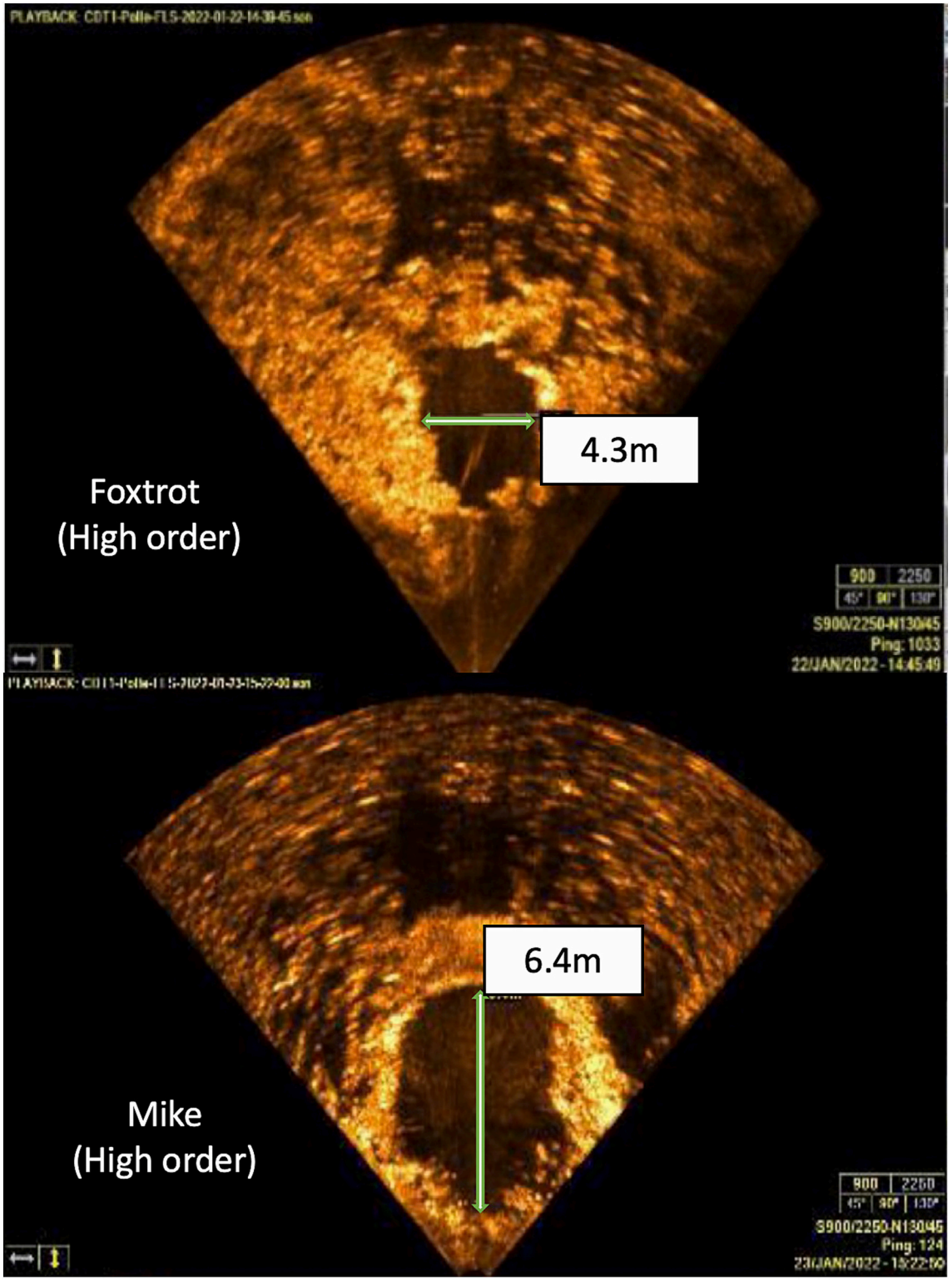

Fig. 18. Diver sonar scan images of UXO's FOXTROT & MIKE after high-ordered clearance events. The upper image is from FOXTROT (~200 kg + 10 kg donor charge) sonar scan image in 16.9 m water depth, sensor heading 159° with a − 7° pitch angle and MIKE (~170 kg + 10 kg donor charge) in 18.5 m water depth on heading 293° and − 2° pitch.

bandwidths used were felt to be a reasonable compromise of computational efficiency, and accuracy however the consideration of wider bandwidths and more detailed sediment modelling could be considered in future work to improve on this understanding.

In the case of the low-order clearances measured the acoustic output appears to be essentially consistent with the low-order deflagration charges on their own with little or no contribution from the historic charge detonating or observable effect from the deflagration combustion process. As previously observed, the low-order charges are also significantly smaller, in this trial 0.25 kg, and therefore generate lower levels observed than the equivalent use of (for example) a 10 kg donor and any contribution from detonation of the associated historic charge. These

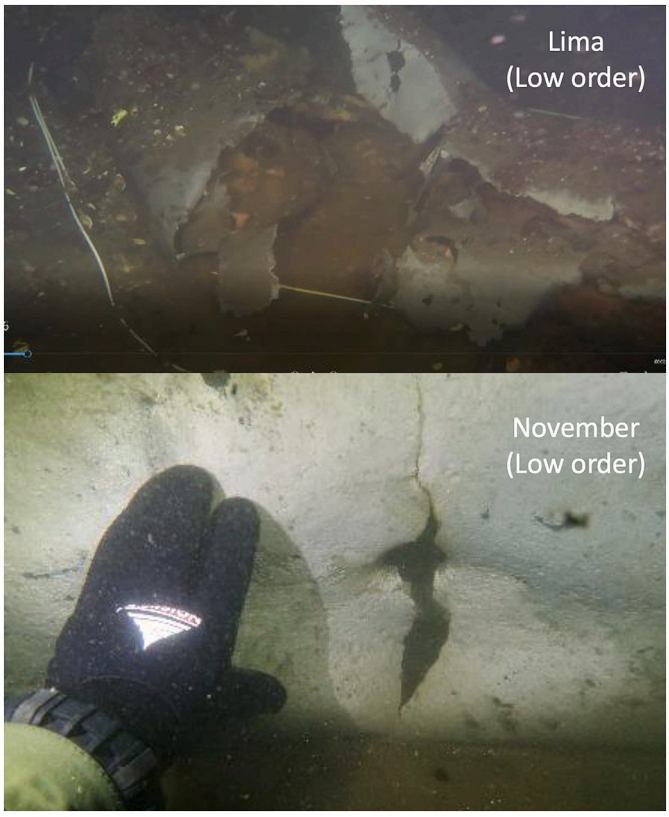

Fig. 19. Post clearance of images of two low-order events LIMA and NOVEMBER showing impact of low-order deflagration on the mine casing.

data again align well with acoustic levels measured from low-order deflagration and high-order donor equivalent measurements reported by Robinson et al., 2020.

Fig. 21 also shows the relative consistency and predictability of the low-order events compared with greater variability potential of the high-order as well as the consistency in the potential reductions in level *versus* range seen during these measurements. Typical reduction in levels of 15–20 dB for both SEL and $L_{p,pk}$ metrics for the use of high to lower order methodologies observed in these measurements have the potential to be even greater if a UXO was to high-order at its full potential. Taking the example of the modelled level of one of the largest UXO in the Great Belt trials of 430 kg, in this case a reduction of between 35 dB and 40 dB could be observed between an equivalent high-order and successful low-order deflagration clearance of the same UXO.

In another independent study in 2020, deflagration was carried out on one of the largest conventional explosive bombs from WWII (a British Tallboy of almost 3600 kg of TNT-eq). In this case a partial deflagration is reported to have resulted in an estimated 55–60 % combustion of the explosives, though unfortunately no acoustic measurements have been reported [Mietkiewicz, 2022].

Another non-acoustic consideration in the evaluation of the comparison of the use of high and low-order methodologies is the potential for seabed and sediment damage. This may be of particular importance to a wide range of aquatic species particularly with sensitivity to particle motion and vibration components of the propagating energy from these events. High-order events have shown the potential for significant disturbance of the seabed with measurements of significant seabed vibration components at ranges in excess of 2 km both in vertical and horizontal directions and significant long-term disruption / distribution of sediment and UXO material from cratering and debris fields. Similar seabed 'blast marks' have been reported by Garlan *et al,* that they attribute to the explosion of air-dropped ordnance during WWII in the region of Toulon off the coast of France. In this case a significant pro-

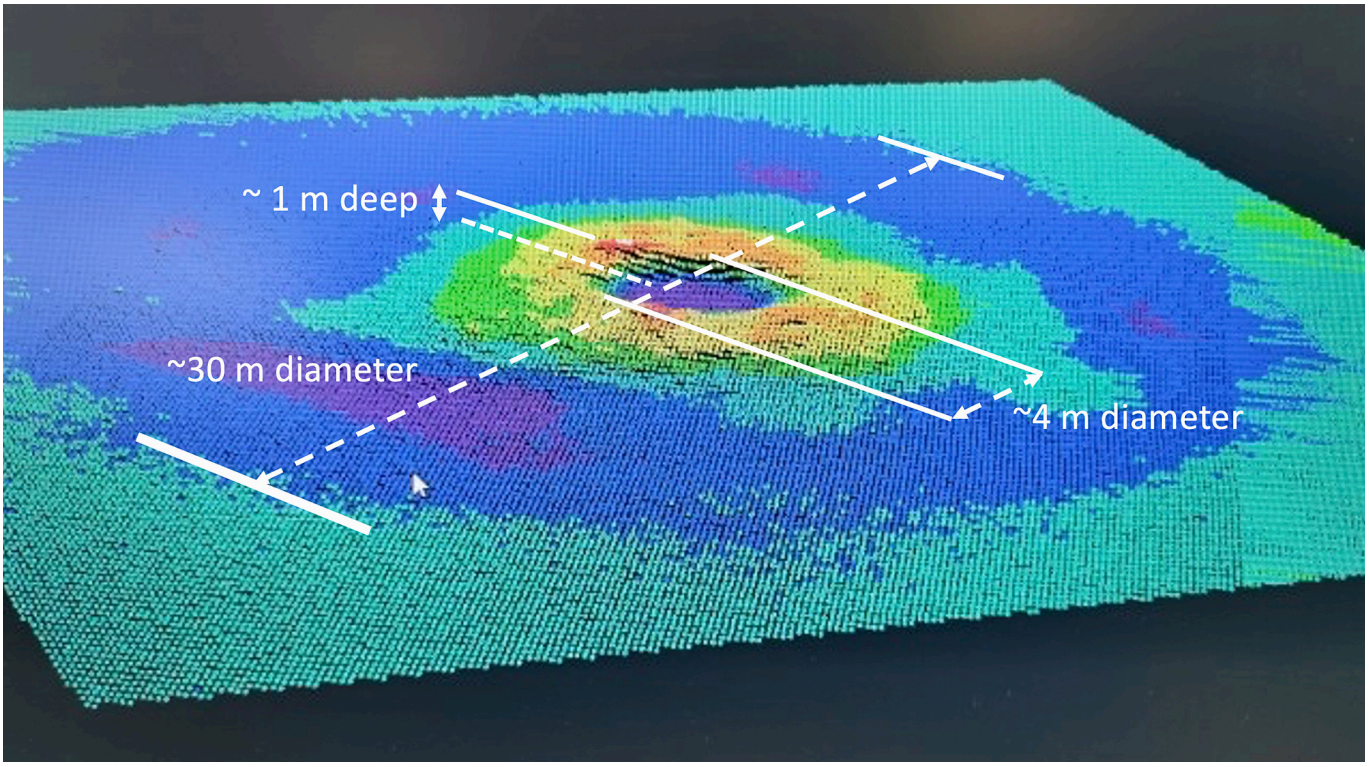

Fig. 20. Multibeam survey of the crater site for the high-order FOXTROT clearance event. The centre crater is estimated to be around 4 m diameter and 1 m deep [Pers. comms, Danish Navy].

Table 6
Estimated ranges of minimum distance in km for avoidance of exceeding PTS impulsive sound peak and weighted SEL criteria for different functional hearing groups from Southall et al., 2019. [Low Frequency (LF), High Frequency (HF), Very High Frequency (VHF) and Pinniped in Water (PW)].

ID	Estimated minimum distance from source to below PTS impact threshold (km)							
	Peak impact criteria (unweighted)				SEL impact criteria (weighted)			
	LF	HF	VHF	PW	LF	HF	VHF	PW
LIMA (LO)	0.21 ± 0.16	0.03 ± 0.03	1.16 ± 0.53	0.29 ± 0.2	0.26 ± 0.11	0.02 ± 0.01	1.03 ± 0.34	0.10 ± 0.05
MIKE (HO)	1.5 ± 0.2	0.6 ± 0.1	4.0 ± 0.4	1.6 ± 0.3	2.1 ± 0.6	0.3 ± 0.1	4.7 ± 1.1	1.0 ± 0.3

Table 7
Estimated ranges of the minimum distance km for avoidance of exceeding TTS impulsive sound peak and weighted SEL criteria for different functional hearing groups from Southall et al., 2019. [Low Frequency (LF), High Frequency (HF), Very High Frequency (VHF) and Pinniped in Water (PW)].

ID	Estimated minimum distance from source to below TTS impact threshold (km)							
	Peak impact criteria (unweighted)				SEL impact criteria (weighted)			
	LF	HF	VHF	PW	LF	HF	VHF	PW
LIMA (LO)	0.39 ± 0.27	0.12 ± 0.12	1.77 ± 0.74	0.57 ± 0.32	1.5 ± 0.5	0.2 ± 0.1	3.9 ± 0.8	0.8 ± 0.3
MIKE (HO)	2.2 ± 0.2	1.0 ± 0.1	6.3 ± 1.0	2.4 ± 0.2	6.7 ± 1.5	1.6 ± 0.5	13.1 ± 2.2	3.9 ± 0.8

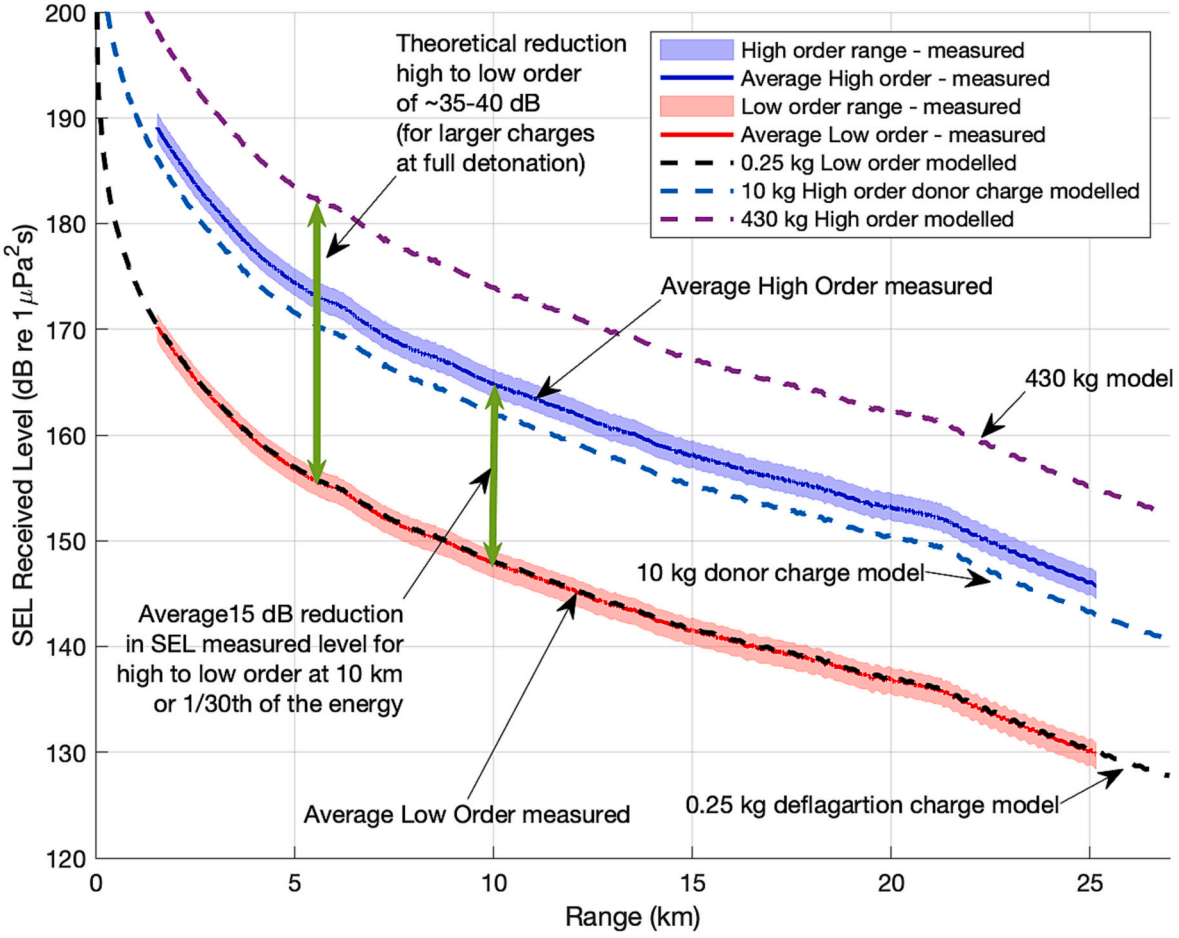

Fig. 21. Summary of SEL acoustic levels measured and modelled *versus* range comparing high and low-order acoustic levels.

portion of the seabed, up to 15.8 %, is covered by craters with diameters ranging from 11 to 134 m. Note that these marks observed in 2018 have been thought to have remained in the interim decades due to of a general absence of sedimentary dynamics and of the trawling by the fishermen in this location [Garlan et al., 2018] which may in other locations reduce their presences over time. By comparison the low-order events measured in the current study generated significantly less to no seabed disturbance with effects often localized to within a few meters of the original UXO directly after the EOD event.

Another important consideration is chemical contamination both prior, during and post clearance from explosive material contributions. Several of the UXO considered in this trial were severely corroded with

explosive material directly exposed to the environment, potentially for many years. Changes in the viability or sensitivity of UXO materials due to long term exposure to saline environments is discussed by Pfeiffer [Pfeiffer, 2012] as well as potential negative environmental impacts due to chemical toxicity by a number of active research programs *e.g.* [Strehse et al., 2017; den Otter et al., 2023, Maser *et al,* 2023]. Concerns highlighted from toxic contamination from *in situ* UXO's may act as another driver for promotion of clearance of these UXO to remove the long-term contamination potential.

In consultation with the Danish Navy EOD experts involved in this study all the clearance operations carried out were in their opinion successful and the associated weapons could be considered safe from risk of further detonations from their EOD perspective. It is also noted that particularly in the case of a low-order deflagration, the process may not consume all explosive material and some larger pieces of this material may be left *in situ* as well as the possibility of micro level chemical contamination in the surrounding water column and sediments. The risks associated with for example, the collection and retrieval of these residuals and/or longer-term chemical contamination from residuals left *in situ* are still unknown and warrant further investigation. Proponents of low-order deflagration methodologies have argued that remaining UXO debris can be safely collected by divers or Remotely Operated Vehicle (ROV). Preliminary data from this study has shown elevated contamination levels of explosive residues in the vicinity of the low-order deflagration clearance events. By comparison, the highly energetic nature of high-order detonations means that combustion products and residues will be widely distributed throughout the water column and dispersed over a wide area due to tidal movements. Thus, direct comparison of chemical contamination concentrations and footprints between high and low-order methodologies is challenging but worthy of further investigation to inform safe underwater disposal of UXO.

Low-order methods such as described can significantly reduce the acoustic noise impact on aquatic wildlife compared to equivalent high-order methodologies. However, it should be noted that these sources still result in sound levels that can present potential for injury or disturbance at ranges of serval kilometres for some species for example harbour porpoise. We conclude that low-order EOD operations would need to be considered in combination with other mitigation measures strategies such as the use of abatement methodologies *i.e.* bubble curtains or shields, removal methodologies, the use of spatial and temporal restrictions on the activity, passive acoustic monitoring to inform on the presence of animals when vocalizing, [Merchant and Robinson, 2020] to further reduce these risks.

The authors recommend that further *in situ* acoustic measurements (pressure field, seabed vibration and particle velocity) be made of both low-order and high-order methods for comparison, together with assessments of effectiveness and safety of the EOD operation, the safety and requirement of retrieval of residues and extent of chemical contamination from both the EOD process and post process periods for both high and low-order methodologies.

CRediT authorship contribution statement

Paul A. Lepper: Conceptualization, Formal analysis, Investigation, Methodology, Writing – original draft, Writing – review & editing. **Sei-Him Cheong:** Investigation, Methodology, Software, Writing – review & editing, Conceptualization, Formal analysis. **Stephen P. Robinson:** Conceptualization, Methodology, Writing – review & editing. **Lian Wang:** Formal analysis, Investigation, Methodology, Writing – review & editing, Conceptualization, Writing – original draft. **Jakob Tougaard:** Conceptualization, Investigation, Methodology, Writing – review & editing. **Emily T. Griffiths:** Conceptualization, Investigation, Methodology, Writing – review & editing. **John P. Hartley:** Conceptualization, Funding acquisition, Project administration, Writing – original draft, Writing – review & editing.

Declaration of competing interest

The authors declare that they have no known competing financial interests or personal relationships that could have appeared to influence the work reported in this paper.

Data availability

Data will be made available on request.

Acknowledgements

We would like to thank the editor and the eviewers for their invaluable suggestions and insights to the final version of this manuscript. This project was funded by the UK's Department for Business, Energy and Industrial Strategy's Offshore Strategic Environmental Assessment programme under contract OESEA-21-127. The authors would like to sincerely thank Lars Møller-Pedersen and his team from the Royal Danish Navy, Captain Torben Vang and crew members Lars Renvand, Jesper Voetmann, Frank Landkildehus and Michael Bach of the RV Aurora, and Clive Gale for the EOD assessment detail as well as Katrine Juul Andresen for assistance with retrieval of chemical analysis samples.

Appendix A. Supplementary data

Supplementary data associated with this article can be found in the online version, at doi:https://doi.org/10.1016/j.marpolbul.2023.115965. These data include the Google maps of the most important areas described in this article.

References

Ainslie, M., de Jong, C., Robinson, S.P., Lepper, P.A., 2012. What is the Sourcel level of Piledriving noise in water. Advances in Experimental Medicine 730, 445–448. https://doi.org/10.1007/978-1-4419-7311-5_100.

Aker, J., Howard, B., Reid, M., 2012. Risk management for unexploded ordinance (UXO) in the marine environment. Dalhousie Journal of Interdisciplinary Management 8. Available from: djim.management.dal.ca https://doi.org/10.5931/djim.v8i2.366.

Albright, R.D., 2012. Cleanup of Chemical and Explosive Munitions, Second edition. William Andrew Publishing, ISBN 9781437734775, pp. 165–170. https://doi.org/10.1016/B978-1-4377-3477-5.00012.

Appel, D., Strehse, J.S., Martin, H.-J., Maser, E., 2018. Bioaccumulation of 2,4,6-trinitrotoluene (TNT) and its metabolites leaking from corroded munition in transplanted blue mussels (M. Edulis). Mar. Pollut. Bull. 135, 1072–1078.

Arons, A.B., 1954. Underwater explosion shock wave parameters at large distances from the charge. J. Acoust. Soc. Am. 26, 343–346.

Arons, A.B., 1970. Evolution of explosion pressure-wave characteristics in the region relatively close to origin. J. Acoust. Soc. Am. 47, 91.

BEIS, 2020. Protocol for in-situ underwater measurement of explosive ordnance disposal for UXO. In: Cheong, S.-H., Wang, L., Lepper, P.A., Robinson, S.P. (Eds.), Offshore energy SEA sub-contract OESEA-19-107. Available from: link.

von Benda-Beckmann, A.M., Aarts, G., Sertlek, H.O., Lucke, K., Verboom, W.C., Kastelein, R.A., Ketten, D.R., van Bemmelen, R., Lam, F.A., Kirkwood, R.J., Ainslie, M.A., 2015. Assessing the impact of underwater clearance of unexploded ordnance on harbour porpoises (*Phocoena phocoena*) in the southern North Sea. Aquat. Mamm. 41 (4), 503–523.

Binnerts, B., de Jong, C.A.F., Karasalo, I., Östberg, M., Folegot, T., Clorenneq, D., Ainslie, M.A., Warner, G., Wang, L., 2019. Model benchmarking results for ship noise in shallow water. In: Proceedings of the 5th Underwater Acoustics Conference and Exhibition UACE2019. Greece, Hersonissos, Crete.

Chapman, N.R., 1985. Measurement of the waveform parameters of shallow explosive charges. J. Acoust. Soc. Am. 78, 672–681.

Chapman, N.R., 1988. Source levels of shallow explosive charges. J. Acoust. Soc. Am. 84, 697–702.

Cheong, S.-H., Wang, L., Lepper, P.A., Robinson, S.P., 2020. Characterisation of acoustic fields generated by UXO removal, phase 2. In: Offshore Energy SEA Sub-Contract OESEA-19-107, NPL Report AC 19. Available from: link.

Cole, R.H., 1948. Underwater Explosions. Princeton University Press, Princeton, NJ.

Collins, M.D., 1993. A split-step Padé solution for the parabolic equation method. J. Acoust. Soc. Am. 93, 1736–1742. https://doi.org/10.1121/1.406739.

Cooper, P.W., 1996. Explosives Engineering. Wiley-VCH, ISBN 0-471-18636-8.

Cottrell, L., Dupuy, K., 2021. Alternatives to Open Burning and Open Detonation: The Disparity Between HMA and Commercial Best Practices. The Journal of Conventional Weapons Destruction 25 (1). Article 22. Available at: https://commons.lib.jmu.edu/cisr-journal/vol25/iss1/22.

Croci, K., Arrigoni, M., Boyce, P., Gabillet, C., Grandjean, H., 2014. Mitigation of underwater explosion effects by bubble curtains : experiments and modelling. In: 23rd MABS (Military Aspects of Blast and Shock), Oxford, UK, p. 14. Sep 2014, United Kingdom. https://hal.archives-ouvertes.fr/hal-01071652/.

Dahl, P.H., Jenkins, A.K., Casper, B., Kotecki, S.E., Bowman, V., Boerger, C., Dall'Osto, D. R., Babina, M.A., Popper, A.N., 2020. Physical effects of sound exposure from underwater explosions on Pacific sardines (*Sardinops sagax*). J. Acoust. Soc. Am. 147 (4), 2383–2395.

Danil, K., St. Leger, J.A., 2011. Seabird and dolphin mortality associated with underwater detonation exercises. Mar. Technol. Soc. J. 45, 89–95. https://doi.org/10.4031/mtsj.45.6.5.

Davies, G., 1996. Munitions dump explodes into headlines again. Mar. Pollut. Bull. 32 (3), 250–251.

Detloff, K., Ludwichowski, I., Deimer, P., Schütte, H.-J., Karlowski, U., Koschinski, S., 2012. Environmental nongovernmental Organizations' perspective on underwater munitions. Mar. Technol. Soc. J. 46 (1), 11–16.

Domenico, S.N., 1982. Acoustic wave propagation in air-bubble curtains in water—part I: history and theory. Geophysics 47, 345–353. https://doi.org/10.1190/1.1441340.

Eitner, J., Tröster, S., 2018. "Hazardous contaminated sites in the north and the Baltic Sea", *research news RN08*, Fraunhofer Institute for chemical technology, Munich. Available from: www.Fraunhofer.de.

Favretto-Cristini, N., Garlan, T., Morio, O., Demoulin, X., 2022a. Assessment of risks induced by countermining unexploded large-charge historical ordnance in a shallow water environment—part I: real case study. IEEE J. Ocean. Eng. 47 (2), 350–373. https://doi.org/10.1109/JOE.2021.3111819.

Favretto-Cristini, N., Wang, F., Cristini, P., Garlan, T., Morio, O., Mercerat, E.D., Monteiller, V., Deschamps, A., Beucler, E., 2022b. Assessment of risks induced by countermining unexploded large-charge historical ordnance in a shallow water environment—part II: modeling of seismo-acoustic wave propagation. IEEE J. Ocean. Eng. 47 (2), 374–398. https://doi.org/10.1109/JOE.2021.3111791.

Finneran, J.J., Jenkins, A.K., 2012. Criteria and Thresholds for U.S. Navy Acoustic and Explosive Effects Analysis. SSC Pacific, San Diego, CA. Available from: https://apps.dtic.mil/sti/pdfs/ADA561707.pdf.

Finneran, J.J., Schlundt, C.E., Carder, D.A., Clark, J.A., Young, J.A., Gaspin, J.B., 2000. Auditory and behavioral responses of bottlenose dolphins (*Tursiops truncatus*) and white whales (*Delphinapterus leucas*) to impulsive sounds resembling distant signatures of underwater explosions. J. Acoust. Soc. Am. 108, 417–431.

Garlan, T., Mathias, X., Brenon, E., Favretto-Cristini, N., Deschamps, A., Beucler, E., Guyomard, P., Morio, O., et al., 2018. Circular sedimentary figures of anthropic origin in a sediment stability context. J. Coast. Res. 85 https://doi.org/10.2112/SI85-005.1.

Gaspin, J.B., Goertner, J.A., Blatstein, I.M., 1979. The determination of acoustic source levels for shallow underwater explosions. J. Acoust. Soc. Am. 66, 1453–1462.

Gitterman, Y., 2009. Near-source audiovisual, hydroacoustic, and seismic observations of Dead Sea underwater explosions. Combustion, explosion, and Shock Waves 45 (2), 218–229. https://doi.org/10.1007/s10573-009-0029-1.

Gupta, R., Kumar, M., Singh, S.K., Singla, G.K., Narang, R., 2022. Deflagration to Detonation Transition in Cast Explosives: Revisiting the Classical Model. In: Prop., Explos., Pyrotech, 47, e202100284. https://doi.org/10.1002/prep.202100284.

Hamilton, E.L., 1980. Geoacoustic modeling of the seafloor. J. Acoust. Soc. Am. 68, 1313–1340.

Hannay, B., Chapman, N.R., 1999. Source levels for shallow underwater sound charges. J. Acoust. Soc. Am. 105 (1), 260–263.

Hawkins, A.D., Hazelwood, R.A., Popper, A.N., Macey, P.C., 2021. Substrate vibrations and their potential effects upon fishes and invertebrates. J. Acoust. Soc. Am. 149 (4), 2782–2790.

Hazelwood, R.A., Macey, P.C., 2021. Noise waveforms within seabed vibrations and their associated evanescent sound fields. J. Mar. Sci. Eng. 2021 (6), 61. https://doi.org/10.3390/jmse9070733.

Hazelwood, R.A., Macey, P.C., Robinson, S.P., Wang, L.S., 2018. Optimal transmission of interface vibration wavelets – a simulation of seabed seismic responses. J. Mar. Sci. Eng. 2018 (9), 733. https://doi.org/10.3390/jmse6020061.

IEC 60565-1, 2020. Underwater acoustics – Hydrophones – Calibration of hydrophones – Part 1: Procedures for free-field calibration of hydrophones, International Electrotechnical Commission, Geneva, Switzerland.

IEC 60565-2, 2019. Underwater acoustics – Hydrophones – Calibration of hydrophones –Part 2: Procedures for low frequency pressure calibration, International Electrotechnical Commission, Geneva, Switzerland.

ISO 18405, 2017. Underwater Acoustics – Terminology, ISO (the International Organization for Standardization), Switzerland, 2017.

ISO 18406, 2017. Underwater Acoustics – Measurement of Radiated Underwater Sound from Percussive Pile Driving, ISO (the International Organization for Standardization), Switzerland, 2017.

Jenkins, A.K., Dahl, P.H., Kotecki, S.E., Bowman, V., Casper, B., Boerger, C., Popper, A. N., 2022. Physical effects of sound exposure from underwater explosions on Pacific mackerel (*Scomber japonicus*): effects on non-auditory tissues. J. Acoust. Soc. Am. 151 (6), 3947–3956.

JNCC, 2010. JNCC guidelines for minimising the risk of injury to marine mammals from using explosives (August 2010). Available: www.jncc.gov.uk.

Ketten, D.R., Lien, J., Todd, S., 1993. Blast injury in humpback whale ears: evidence and implications. J. Acoust. Soc. Am. 94, 1849–1850. https://doi.org/10.1121/1.407688.

Koschinski, S., 2011. Underwater noise pollution from munitions clearance and disposal, possible effects on marine vertebrates, and its mitigation. Mar. Technol. Soc. J. 45 (6), 80–88.

Koschinski, S., Kock, K.H., 2009. Underwater unexploded ordnance - methods for a cetacean-friendly removal of explosives as alternatives to blasting. In: Reports Int. Whal. Comm. SC/61 E. https://literatur.thuenen.de/digbib_extern/dk041983.pdf.

Koschinski, S., Kock, K.H., 2015. "Underwater Unexploded Ordnance - Methods for a Cetacean-Friendly Removal of Explosives as Alternatives to Blasting", 22nd ASCOBANS Advisory Committee Meeting.

Lippert, S., Nijhof, M., Lippert, T., Wilkes, D., Gavrilov, A., Heitmann, K., Ruhnau, M., von Estorff, O., Schäfke, A., Schäfer, I., Ehrlich, J., MacGillivray, A., Park, J., Seong, W., Ainslie, M.A., de Jong, C., Wood, M., Wang, L., Theobald, P., 2016. COMPILE—A generic benchmark case for predictions of marine pile-driving noise. IEEE J. Ocean. Eng. 41 (4), 1061–1071. Oct. 2016. https://doi.org/10.1109/JOE.2016.2524738.

Loye, D.P., Arndt, W.F., 1948. A sheet of ar bubble as an acoustic screen for underwater noise. J. Acoust. Soc. Am. 20 (2), 143–145.

MARTA, 2023. MARTA - the GEUS metadata base of shallow geophysical data, GEUS archives. Bekendtgørelse af lov om råstoffer Lovbekendtgørelse nr 950 af 24/09/2009. URL: https://data.geus.dk/geusmapmore/marta/guide_marta.html. last accessed 11th December 2023.

Martin, S.B., Barclay, D.R., 2019. Determining the dependence of marine pile driving sound levels on strike energy, pile penetration, and propagation effects using a linear mixed model based on damped cylindrical spreading. J. Acoust. Soc. Am. 146 (1), 109–121. https://doi.org/10.1121/1.5114797, 1 July 2019.

Maser, E., Ahdresen, K.J., BÜnning, T.H, Clausen, O.R., Wichert, U., Strehse, J.S., 2023. Ecotoxicological Risk of World War Relic Munitions in the Sea after Low- and High-Order Blast-in-Place Operations. Environ. Sci. Technol. 57, 48. https://doi.org/10.1021/acs.est.3c04873.

Maser, E., Strehse, J.S., 2020. Don't blast: blast-in-place (BiP) operations of dumped world war munitions in the oceans significantly increase hazards to the environment and the human seafood consumer. Arch. Toxicol. 13.

Meins, O., Aimone-Martin, C., Meins, B., 2019. Influence of sample rate on blast pressure measurments. J. Explos. Eng. Sep-Oct, 29–35.

Merchant, N.D., Robinson, S.P., 2020. "Abatement of underwater noise pollution from pile-driving and explosions in UK waters". Report of the UKAN noise abatement workshop, 12 NOVEMBER 2019 at the Royal Society, London. https://doi.org/10.6084/m9.figshare.11815449.

Merchant, N.D., Andersson, M.H., Box, T., Le Courtois, F., Cronin, D., Holdsworth, N., Kinneging, N., Mendes, S., Merck, T., Mouat, J., Norro, A.M.J., Ollivier, B., Pinto, C., Stamp, P., Tougaard, J., 2020. Impulsive noise pollution in the Northeast Atlantic: Reported activity during 2015–2017. Mar. Pollut. Bull. 152. https://doi.org/10.1016/j.marpolbul.2020.110951.

Mietkiewicz, R., 2022. High explosive unexploded ordnance neutralization - tallboy air bomb case study. Defence Technology 18, 524–535.

Mitra, Sanjit K., 2001. Digital Signal Processing: A Computer-Based Approach, 2nd Ed. McGraw-Hill, New York.

NMFS, 2018. "Revisions to Technical Guidance for Assessing the Effects of Anthropogenic Sound on Marine Mammal Hearing", *NOAA Technical Memorandum NMFS-OPR- 59*, 167p. NOAA, US Dept. of Commer.

NOAA, 2016. Independent peer review reports of underwater calculator for shocks or UWCv2 (Vers 2.0), Dahl. P. US National Ocean and atmospheric administration (NOAA), Center for Independent Experts. Available from. www.https://www.st.nmfs.noaa.gov/Assets/Quality-Assurance/documents/peer-review-report.

Novik, G.P., Abrahamsen, E.B., Sommer, M., 2023. Improving the decision making basis by strengthening the risk assessments of unexploded ordnance and explosive remnants of war. Saf. Sci. 160 (2023), 106065. ISSN 0925-7535. https://doi.org/10.1016/j.ssci.2023.106065.

Nowak, P.R., Gajewski, T., Peksa, P., Sielicki, P.W, 2022. Experimental verification of different analytical approaches for estimating underater explosives. Int. J. Prot. Struct. 14 (4), 571–583. https://doi.org/10.1177/20414196221120511.

den Otter, J.H., Pröfrock, D., Bünning, T.H., Strehse, J.S., van der Heijden, A.E.D.M., Maser, E., 2023. Release of ammunition-related C ompounds from a Dutch marine dump site. Toxics 11, 238. https://doi.org/10.3390/toxics11030238.

Parsons, E.C.M., Birks, I., Evans, P.G.H., Gordon, J.C.D., Shrimpton, J.H., Pooley, S., 2000. The possible impacts of military activity on cetaceans in West Scotland. European Research on Cetaceans 14, 185–190.

Patent WO 03/058155 A1, 2003. International Patent "Device for Disruption of Explosive Ordnance", 17 July 2003.

Pedersen, A., 2002. *"Low-Order Underwater Detonation"*, ESTCP *Report UX-0104*. Environmental Security Technology Certification Program, U.S. Department of Defense. Available from: https://apps.dtic.mil/sti/tr/pdf/ADA603983.pdf.

Pfeiffer, F., 2012. "Changes in Properties of Explosives Due to Prolonged Seawater Exposure", *Marine Technology Society Journal*, 102–110. https://doi.org/10.4031/MT SJ.46.1.5.

Popper, A.N., Hawkins, A.D., Fay, R.R., Mann, D.A., Bartol, S., Carlson, T.J., Coombs, S., Ellison, W.T., Gentry, R.L., Halvorsen, M.B., Løkkeborg, S., Rogers, P.H., Southall, B. L., Zeddies, D.G., Tavolga, W.N., 2014. "Sound exposure guidelines for fishes and sea turtles: A technical report" ASA S3/SC1.4 TR-2014, ANSI accredited standards committee S3/SC1, American National Standards Institute, 2014. https://doi.org/10.1007/978-3-319-06659-2.

Robinson, S.P., Theobald, P.D., Lepper, P.A., 2012. Underwater noise generated from marine piling. Proc. Mtgs. Acoust 2 July 2012 (17 (1)), 070080. https://doi.org/10.1121/1.4790330.

Robinson, S.P., Lepper, P.A., Hazelwood, R.A., 2014. "Good practice for underwater noise measurement", NPL good practice guide no. 133. In: National Measurement Office. The Crown Estate, Marine Scotland. ISSN: 1368-6550. Available from: https://www.npl.co.uk/gpgs/underwater-noise-measurement.

Robinson, S.P., Wang, L., Cheong, S.-H., Lepper, P.A., Marubini, F., Hartley, J.P., 2020. Underwater acoustic characterisation of unexploded ordnance disposal using deflagration. Mar. Pollut. Bull. 160, 111646.

Robinson, S.P., Wang, L., Cheong, S.-H., Lepper, P.A., Hartley, J.P., Thompson, P.M., Edwards, E., Bellmann, M., 2022. Acoustic characterisation of unexploded ordnance disposal in the North Sea using high order detonations. Mar. Pollut. Bull. 184, 114178.

Salomons, E.M., Binnerts, B., Betke, K., von Benda-Beckmann, A.M., 2021. Noise of underwater explosions in the North Sea. A comparison of experimental data and model predictions. J. Acoust. Soc. Am. 149 (3), 1878–1888.

Sayle, S., Windeyer, T.C.M., Conrod, S., Stephenson, M., 2009. Site assessment and risk management framework for underwater munitions. Mar. Technol. Soc. J. 43 (4), 41–51. https://doi.org/10.4031/MTSJ.43.4.10.

Schmidtke, E.B., 2010. Schockwellendämpfung mit einem Luftblasenschleier zum Schutz der Meeressäuger. In: (Shock wave damping with an air bubble curtain to protect marine mammals), Proceedings of DAGA, pp. 689–690. Berlin, March 2010. http://pub.degaakustik.de/DAGA_2010/data/articles/000140.pdf.

Schmidtke, E.B., 2012. Schockwellendämpfung mit einem Luftblasenschleier im Flachwasser. In: (Shock wave damping with an air bubble curtain in shallow water), Proceedings of DAGA, pp. 949–950. Darmstadt, March 2012. http://pub.degaakustik.de/DAGA_2012/data/articles/000332.pdf.

Schmidtke, E.B., Nutzul, B., Ludwig, S., 2009. Risk mitigation for sea mammals – The use of air bubble ahainst shock waves. In: Proceedings of DAGA, 2009, pp. 269–270. Rotterdam.

Schuster, R., Strehse, J.S., Ahvo, A., Turja, R., Maser, E., Bickmeyer, U., Lehtonen, K.K., Brenner, M., 2021. Exposure to dissolved TNT causes multilevel biological effects in Baltic mussels (Mytilus spp.). Mar. Environ. Res. 167 (2021), 105264. ISSN 0141-1136. https://doi.org/10.1016/j.marenvres.2021.105264.

Sercel, 2023. GPR1500 data sheet. available online. https://www.sercel.com/products/Pages/GPR.aspx.

Sertlek, H.O., Slabbekoorn, H., ten Cate, C., Ainslie, M.A., 2019. Source specific sound mapping: spatial, temporal and spectral distribution of sound in the Dutch North Sea. Environ. Pollut. 247, 1143–1157.

Siebert, U., Stürznickel, J., Schaffeld, T., Oheim, R., Rolvien, T., Prenger-Berninghoff, E., Wohlsein, P., Lakemeyer, J., Rohner, Schick, S. Aroha, Gross, L., Nachtsheim, S., Ewers, D., Becher, C., Amling, P., Morell, M., 2022. "Blast Injury on Harbour Porpoises (*Phocoena phocoena*) from the Baltic Sea after Explosions of Deposits of World War II Ammunition" *Environment International*, **159**, 107014. https://doi.org/10.1016/j.envint.2021.107014.

Skretting, A., Leroy, C.C., 1971. Sound attenuation between 200 Hz and 10 kHz. J. Acoust. Soc. Am. 49, 276.

Smith, M.E., Accomando, A.W., Bowman, V., Casper, B., Dahl, P.H., Kotecjis, Jenkins A. K., Popper, A.N., 2022. Physical effects of sound exposure from underwater explosions on Pacific mackerel (*Scomber japonicus*): effects on the inner ear. J. Acoust. Soc. Am. 152 (2), 733–744. https://doi.org/10.1121/10.0012991.

Soloway, A.G., Dahl, P.H., 2014. Peak sound pressure and sound exposure level from underwater explosions in shallow water. J. Acoust. Soc. Am. 136 (3), El218–223.

Southall, B.L., Finneran, J.J., Reichmuth, C., Nachtigall, P.E., Ketten, D.R., Bowles, A.E., Ellison, W.T., Nowacek, D.P., Tyack, P.L., 2019. Marine mammal noise exposure criteria: updated scientific recommendations for residual hearing effects. Aquat. Mamm. 45 (2), 125–232. https://doi.org/10.1578/AM.45.2.2019.125.

Straume, E.O., Gaina, C., Medvedev, S., Hochmuth, K., Gohl, K., Whittaker, J.M., Fattah, A., Doornenbal, J.C., Hopper, J.R., 2019. GlobSed: updated total sediment thickness in the world's oceans. In: Geochemistry, Geophysics, Geosystems, p. 20. https://doi.org/10.1029/2018GC008115.

Strehse, J.S., Appel, D., Geist, C., Martin, H.-J., Maser, E., 2017. Biomonitoring of 2,4,6-trinitrotoluene and degradation products in the marine environment with transplanted blue mussels (*M. Edulis*). Toxicology 390, 117–123.

Sundermeyer, J.K., Lucke, K., Dähne, M., Gallus, A., Krügel, K., Siebert, U., 2012. Effects of underwater explosions on presence and habitat use of harbor porpoises in the German Baltic Sea. In: Popper, A.N., Hawkins, A. (Eds.), The Effects of Noise on Aquatic Life. Advances in Experimental Medicine and Biology, 730. Springer, New York, NY. https://doi.org/10.1007/978-1-4419-7311-5_64.

Todd, S., Stevick, P., Lien, J., Marques, F., Ketten, D., 1996. Behavioral effects of exposure to underwater explosions in humpback whales (*Megaptera novaeangliae*). Can. J. Zool. 74, 1661–1672.

Weston, D., 1960. Underwater explosions as acoustic sources. Proc. Phys. Soc. 76, 233–249.

Yelverton, J.T., Richmond, D.R., Fletcher, E.R., Jones, R.K., 1973. "Safe Distances from Underwater Explosions for Mammals and Birds", Lovelace Foundation for Medical Education and Research, Albuquerque NM 87108, AD-766 952.